

Factorized Fusion Shrinkage for Dynamic Relational Data

Peng Zhao, Anirban Bhattacharya, Debdeep Pati and Bani K. Mallick
Department of Statistics, Texas A&M University

October 4, 2022

Abstract

Modern data science applications often involve complex relational data with dynamic structures. An abrupt change in such dynamic relational data is typically observed in systems that undergo regime changes due to interventions. In such a case, we consider a factorized fusion shrinkage model in which all decomposed factors are dynamically shrunk towards group-wise fusion structures, where the shrinkage is obtained by applying global-local shrinkage priors to the successive differences of the row vectors of the factorized matrices. The proposed priors enjoy many favorable properties in comparison and clustering of the estimated dynamic latent factors. Comparing estimated latent factors involves both adjacent and long-term comparisons, with the time range of comparison considered as a variable. Under certain conditions, we demonstrate that the posterior distribution attains the minimax optimal rate up to logarithmic factors. In terms of computation, we present a structured mean-field variational inference framework that balances optimal posterior inference with computational scalability, exploiting both the dependence among components and across time. The framework can accommodate a wide variety of models, including dynamic matrix factorization, latent space models for networks and low-rank tensors. The effectiveness of our methodology is demonstrated through extensive simulations and real-world data analysis.

1 Introduction

Relational data describes the relationship between two or more sets of variables and is typically observed as matrices or multi-way arrays/tensors. One of the objectives of relational data analysis is to explain the variation in the entries of a relational array through unobserved explanatory factors. For example, given matrix-valued data $\mathbf{Y} \in \mathbb{R}^{n \times p}$, the static low-rank plus noise model of the form $\mathbf{Y} = \mathbf{U}\mathbf{V}' + \mathbf{E}$, where $\max\{\text{rank}(\mathbf{U}), \text{rank}(\mathbf{V})\} \ll \min\{n, p\}$ and \mathbf{E} is error term, has been extensively studied; see Hoff (2007); Chatterjee (2015); Gavish and Donoho (2014); Donoho et al. (2020) for a flavor and connections with truncated singular value decompositions.

Recent decades have seen a rapidly growing interest in analyzing dynamic, complex data sets in the era of data science. Models for dynamic relational data have found wide applications in numerous practical areas, including dynamic social network analysis (Sarkar and Moore, 2005; Zhu et al., 2016), subspace tracking (Doukopoulos and Moustakides, 2008), traffic prediction (Tan et al., 2016; Chen et al., 2019), recommendation system (Nasiri et al., 2014; Zhang et al., 2021) among others. Compared to static relational data, additional challenges are posed when the observation matrices possess a dynamic structure. Critically, modeling the evolution of $\mathbf{Y}_t, t = 1, \dots, T$ over time is vital. This is commonly achieved by specifying a parsimonious probability model for \mathbf{Y}_t involving lower-dimensional latent/hidden variables at each time point t , and then specifying an appropriate evolution of these observations or latent variables over time. For example, the classical vector autoregressive (VAR) model (Lütkepohl, 2013) has been employed to model the evolution of the observations directly; Sarkar and Moore (2005) used an AR(1) type of evolution of the latent factors in the context of latent space models for dynamic networks; Hoff (2011) parameterized time-varying latent factors in terms of static factors with time-varying weights for a three-way tensor model; Hoff (2015) considered a bi-linear autoregressive model and Friel et al. (2016) modeled the evolution by considering evolving observation-related parameters as well as latent factors in a bipartite network model.

Abrupt changes are important examples of non-stationarity, typically observed in systems that undergo regime changes due to an intervention, such as alliances between nations before/after a war (Gibler, 2008), voting records before and after an election Lee et al. (2004), or the impact of protein networks after a treatment (Hegde et al., 2008). In this article, we present a novel shrinkage process for dynamic relational data to handle such abrupt changes in an adaptive manner. Given the dynamic likelihood $\mathbf{Y}_t = \mathbf{U}_t\mathbf{V}_t' + \mathbf{E}_t$, $t = 1, \dots, T$, we introduce the dependence by shrinking the successive differences between the row vectors $\{\mathbf{u}_{it}\}, \{\mathbf{v}_{it}\}$ of $\mathbf{U}_t, \mathbf{V}_t$ to group-wise sparse vectors. In particular, we propose a factorized fusion shrinkage (FFS) prior, where group-wise global-local shrinkage priors on all the transitions of latent factors are applied to promote group-wise fusion structures. The adopted global-local prior has a sufficient mass around zero, allowing it to effectively shrink transitions to zeros while keeping large enough transitions, promoting fusion structures. In addition, all components of the transitions share the same local scales from the prior,

leading to interpretable group-wise shrinkage. The proposed model attempts to account for the dynamic change and dependence across \mathbf{Y}_t by reflecting the piecewise constant changes among the row and column factors, \mathbf{U}_t and \mathbf{V}_t . The symmetric version of the model is also useful for network models, where one requires that $\mathbf{U}_t = \mathbf{V}_t$ for $t = 1, \dots, T$. In addition, we extend the model to tensor data under the CANDECOMP/PARAFAC (Hitchcock, 1927) (CP) type of low-rank structure.

The proposed FFS priors differ substantially from those in literature analyzing dynamic relational data, like AR(1) priors and Gaussian process priors (Sarkar and Moore, 2005; Sun et al., 2012, 2014; Sewell and Chen, 2015, 2017; Zhang et al., 2018). While the above commonly used dynamic priors tend to introduce the smoothness effect among dynamic transitions, FFS priors are designed to introduce the *stopping* and *separation* effects, so that the transitions are either closed to zeros or large. In particular, the stopping effect of FFS priors can significantly enhance the comparisons of posterior latent vectors. As an illustration, we present one simulation example (see subsection 7.3 in the supplement) to illustrate the effect of FFS prior by comparing it with the latent space model with a commonly used normal-inverse-gamma prior to the transitions (IGLSM, e.g., Sewell and Chen (2015)) in the dynamic network settings. Figure 1 shows an example in which only subjects 1 and 2 change over time. With IGLSM, all subjects change in a small magnitude in the estimated latent space, so it is difficult to identify subjects 1 and 2 among all the other subjects, whereas with FFS, only the subjects 1 and 2 change significantly at the correct time point.

In addition, the separation effect of FFS priors contributes to the detection of clusters of the subjects after estimating the latent factors. According to the cluster results, subjects belonging to the same group can reflect their similar effects in generating the relational data. When performing clustering like K -means, the cluster separation $\delta_t = \min_{i \neq j} \|\mathbf{u}_{it} - \mathbf{u}_{jt}\|_2$ for any $\mathbf{u}_{it}, \mathbf{u}_{jt}$ not in the same cluster plays an important role in the difficulty level of the problem (e.g., eigengap for spectral clustering, see Ng et al. (2001)). In general, the larger δ_t is, the easier it is to detect clusters at time t . Then the separation effect of FFS priors is justified by encouraging more separate clusters: Suppose at time t we have $\mathbf{u}_{it} = \mathbf{u}_{jt}$ for subjects i, j and for time $t + 1$, the subject i moves to another cluster while subject j stays the same. Then we have the cluster separation at time $t + 1$ satisfies $\delta_{t+1} \leq \|\mathbf{u}_{j(t+1)} - \mathbf{u}_{i(t+1)}\|_2 = \|\mathbf{u}_{j(t+1)} - \mathbf{u}_{jt}\|_2 = \|D\mathbf{u}_{jt}\|_2$, which accounts for the necessity of shrinking towards larger transitions. In contrast, the priors that introduce smoothness to the transitions tend to impede the separation of the clusters. Overall, the insight behind the model is to explicitly link the transitions of latent positions with the changing of cluster memberships for a subject: a zero transition implies that there has been no change in cluster membership, while a change in cluster membership implies a large transition.

Dynamic shrinkage priors have been studied in a wide range of literature (Frühwirth-Schnatter and Wagner, 2010; Chan et al., 2012; Groen et al., 2013; Nakajima and West, 2013; Kalli and Griffin, 2014; Kowal et al., 2019). In particular, for dynamic linear models, Kowal et al. (2019) proposed a novel dynamic prior for the transitions with temporal adap-

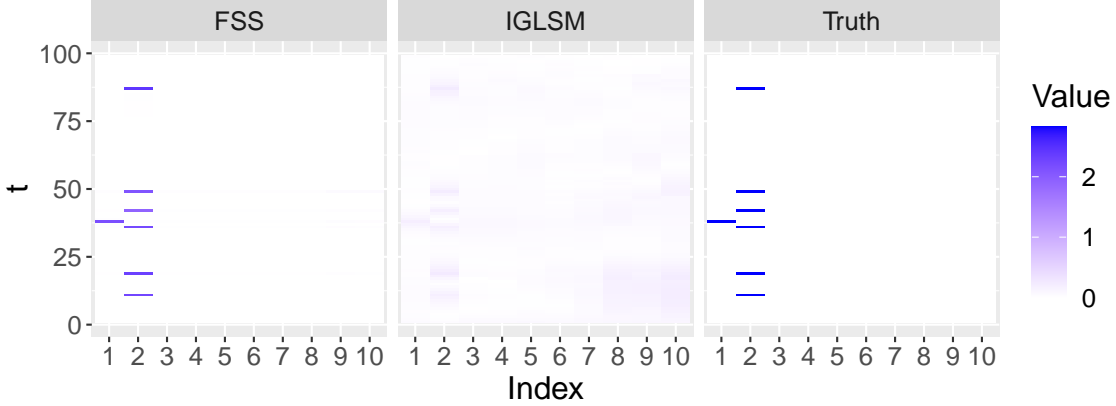


Figure 1: Heatmaps of matrices whose components are ℓ_2 norm of transitions $\{\|\mathbf{D}\mathbf{u}_{it}\|\}_{i=1,\dots,10;t=2,\dots,T}$ after estimating latent vectors by FFS priors, IGLSM and the truth correspondingly. Index: subject index; t : time of the transitions. For IGLSM and FFS prior, Procrustes rotation (5) is performed where the latent vectors of time $t = 2, \dots, T$ are projected to the locations that are most close to its previous locations. FFS priors can better identify the time and subjects of transitions than IGLSM when the true transitions are sparse.

tive local scales for their adopted global-local shrinkage prior. In this article, we consider matrix/tensor valued responses with complex dependence structures using a structural dynamic shrinkage model for the transition of the latent factors and illustrate its applicability across a wide range of problems. Additionally, we provide an in-depth theoretical analysis of the proposed prior.

In dynamic linear or low-rank models, few theoretical investigations into estimation accuracy have been conducted from a Bayesian perspective. We first derive an informative-theoretic lower bound for the model under an appropriate parameter space, incorporating both the initial estimation errors of the matrix/tensor and the selection errors due to the sparsity of the transitions. In addition, we develop an ℓ_1 prior concentration inequality for global-local priors across time when the error rate is also affected by an additional variable other than time due to the multivariate nature of the subjects, improving upon the ℓ_2 prior concentration in the literature; see for example Lemma 1 in [Chakraborty et al. \(2020\)](#). Using the proposed prior concentration and a fractional posterior device, we demonstrate that the posterior under the proposed prior can achieve minimax rates up to logarithmic factors. To our knowledge, both the lower bound and posterior concentration are the first types of results that have been reported in the related literature for dynamic relational data. In addition, it has been established that this fusion type of minimax optimal rate cannot be achieved by a frequentist approach when ℓ_1 -regularization is used ([Fan and](#)

Guan, 2018). Therefore, such near-optimal convergence rates improve upon related models via ℓ_1 penalized approaches. Finally, using dynamic network models as an example, we offer theoretical support to the proposed post-processing technique. While posterior post-processing has been increasingly popular in the Bayesian literature, theoretical validations are comparatively rare; see Lee and Lee (2021) for a recent example in a different context. In particular, community detection and dynamic comparisons are considered under the latent space model, where the truth transitions are assumed to be sparse. Theoretically, we show how the sparsity of the truth transitions and the length of the time range for comparison affect the consistency of the comparison after performing Procrustes rotations. To our knowledge, this is the first study of dynamic networks concerning about long range properties, which quantify the possibility of making comparisons across time when the time range for comparison is a variable that may increase as the number of nodes and time points increases.

From a computational aspect, we present posterior approximations based on variational inference for scalability and computational efficiency while noting that exact MCMC approaches can also be readily developed. We consider a structured mean-field (SMF) variational inference framework, where the group-wise fusion structure, which includes the temporal dependence and the group-wise effect among components, is taken into account. A corresponding coordinate ascent variational inference (Bishop and Nasrabadi (2006), CAVI) algorithm is developed to incorporate the temporal dependence into the variational inference where simple closed-form updatings can be achieved. The proposed algorithm is more efficient than gradient descent or other first-order algorithm types with little increase in the complexity per iteration since the computation can utilize the banded (or block tri-diagonal) structure of the second-order moments, which incurs a $O(Td^3)$ cost for matrix inversion compared to a naive approach with $O(T^3d^3)$ cost. Finally, we extend our SMF variational inference framework to tensor data by utilizing a CP type of low-rank factorization.

2 Methodology

2.1 Factorized Fusion Shrinkage

Let $\mathcal{Y} = [\mathcal{Y}_1, \dots, \mathcal{Y}_T]$, where \mathcal{Y}_t is an M -way tensor $\mathcal{Y}_t \in \mathbb{R}^{n_1 \times \dots \times n_M}$ for $t = 1, \dots, T$. We begin with a general dynamic low-rank tensor model:

$$\mathcal{Y}_t \sim p(\mathcal{M}_t, \beta), \quad \mathcal{M}_t = \sum_{l=1}^d \mathbf{u}_{t,l}^{(1)} \otimes \dots \otimes \mathbf{u}_{t,l}^{(M)}, \quad (1)$$

where \otimes is the vector outer product, \mathcal{M}_t is the mean of \mathcal{Y}_t , $\mathbf{U}_t^{(m)} = [\mathbf{u}_{t,1}^{(m)}, \dots, \mathbf{u}_{t,d}^{(m)}] = [\mathbf{u}_{1t}^{(m)}, \dots, \mathbf{u}_{nt}^{(m)}]'$ and β represents some additional parameters (e.g., variance, subject-specific effects, etc.). When structural changes are caused by interventions, abrupt changes are

typically observed when using dynamic models. For example, the global alliance networks among nations underwent dramatic changes in the late 1940s due to the end of World War II, followed by the sudden formulation of the ‘iron curtain’ (Harbutt, 1988). To handle abrupt changes, we consider the following group-wise fusion structure:

$$\sum_{t=2}^T \sum_{i=1}^{n_m} \{D\mathbf{u}_{it}^{(m)} \neq \mathbf{0}\} \leq s^{(m)}, m = 1, \dots, M \quad (2)$$

with $s^{(m)} \ll n_m T$ and $D\mathbf{u}_{it}^{(m)} = \mathbf{u}_{it}^{(m)} - \mathbf{u}_{i(t-1)}^{(m)}$. The above structure (2) sparsely constrains the total number of transitions in a group-wise manner. In a similar manner to applying the horseshoe prior Carvalho et al. (2009) as a continuous prior to introducing sparsity structures, we adopt a continuous prior that shrinks the posterior towards the above structure (2). To achieve this goal, we propose a factorized fusion shrinkage (FFS) prior, in which group-wise global-local shrinkage priors are utilized in the transition of the latent factors:

$$\begin{aligned} \mathbf{u}_{it}^{(m)} &\sim \mathcal{N}(\mathbf{0}, \sigma_{0i}^{(m)2} \mathbb{I}_d), \quad \sigma_{0i}^{(m)2} \sim \text{IG}(a_{\sigma_0}, b_{\sigma_0}), \quad t = 1. \\ \mathbf{u}_{i(t+1)}^{(m)} | \mathbf{u}_{it}^{(m)} &\sim \mathcal{N}(\mathbf{u}_{it}^{(m)}, \lambda_{it}^{(m)2} \tau_i^{(m)2} \mathbb{I}_d), \quad t = 1, \dots, T-1. \\ \lambda_{it}^{(m)} &\sim \text{Ca}^+(0, 1), \quad \tau_i^{(m)} \sim g, \quad t = 1, \dots, T-1, \end{aligned} \quad (3)$$

for $i = 1, \dots, n_m$, $m = 1, \dots, M$, where $a_{\sigma_0}, b_{\sigma_0}$ are constants. The proposed model adopts a group-wise global-local parameterization, and independent half-Cauchy priors are placed on the local transition scales $\lambda_{it}^{(m)} \sim \text{Ca}^+(0, 1)$, which shrinks small transition vectors towards zero vectors while retaining large transitions. The global prior g is chosen to ensure that the mass around zero is sufficiently large. For example, the horseshoe prior applies $\tau_i^{(m)} \sim \text{Ca}^+(0, 1)$, while Gamma distribution $\tau_i^{(m)2} \sim \Gamma(a_\tau, b_\tau)$ with positive constants a_τ, b_τ can also be adopted. The global-local priors are adopted in a group-wise manner to simultaneously shrink all components of the transition vectors $D\mathbf{u}_{it}^{(m)}$ to sparse vectors, as all the d components of $D\mathbf{u}_{it}^{(m)}$ share the same local scale $\lambda_{it}^{(m)}$ from the prior. In particular, when $M = 2$ and $\mathcal{M}_t = \mathbf{U}_t^{(1)} \mathbf{U}_t^{(2)'}$, if $\{\mathbf{U}_t^{(2)}\}_t$ is specified, then the estimation of $\mathbf{u}_{i.}^{(1)}$ can be viewed as a multivariate regression problem with time-dependent predictors and a group-wise dynamic shrinkage prior, where the time-dependent predictors are represented by a 3-way tensor $\{\mathbf{U}_t^{(2)}\}_t$, and the responses are the i -th columns of \mathcal{Y}_t for all t . Throughout the article, we assume the latent dimension d is known and fixed across all time. Note that although the sparsity constraint (2) is not identifiable for individual $\mathbf{U}_t^{(m)}$, we still aim to recover $\mathbf{U}_t^{(m)}$ through some post-process approaches discussed in Section 2.2.

Two special cases are worth discussing independently. Assuming $M = 2$, the following Gaussian matrix factorization model is worth considering:

$$\mathbf{Y}_t \sim \mathcal{N}(\mathbf{U}_t \mathbf{V}_t', \sigma^2) \quad (4)$$

where $\mathbf{U}_t \in \mathbb{R}^{n \times d}$ and $\mathbf{V}_t \in \mathbb{R}^{p \times d}$ for $t = 1, \dots, T$. Then our proposed prior (3) shrinks the row vectors of \mathbf{U}_t , \mathbf{V}_t towards the following two-sided group-wise fusion structure:

$$\sum_{t=2}^T \sum_{i=1}^n \mathbb{1}\{D\mathbf{u}_{it} \neq \mathbf{0}\} \leq s_u, \quad \text{and} \quad \sum_{t=2}^T \sum_{j=1}^p \mathbb{1}\{D\mathbf{v}_{jt} \neq \mathbf{0}\} \leq s_v,$$

where s_u, s_v are much less than nT and pT respectively.

Additionally, we consider the following latent space model for network data

$$\mathbf{Y}_t \sim \text{Bernoulli}(\text{logistic}(-\mathbf{U}_t \mathbf{U}_t')),$$

where $\mathbf{U}_t \in \mathbb{R}^{n \times d}$ for $t = 1, \dots, T$. Then the prior (3) is applied to shrink the parameters towards structures $\sum_{t=2}^T \sum_{i=1}^n \mathbb{1}\{D\mathbf{u}_{it} \neq \mathbf{0}\} \leq s$, with $s \ll nT$.

Factorized shrinkage offers some advantages over component-wise fusion shrinkage directly on the means $\{\mathcal{M}_t\}_t$: First, FFS priors can reduce the number of effective parameters from npT to $(n+p)dT$ even without considering sparsity, whereas component-wise fusion shrinkage of the means $\{\mathcal{M}_t\}_t$ cannot induce low-rank structures. Furthermore, FFS priors can also introduce component-wise fusion shrinkage on the means $\{\mathcal{M}_t\}_t$, similar to the effects of fused shrinkage directly on the mean matrices $\{\mathcal{M}_t\}_t$. In particular, we examine the property of the marginal prior on the components of $D\mathcal{M}_t = \mathbf{U}_{t+1} \mathbf{V}_{t+1}' - \mathbf{U}_t \mathbf{V}_t'$ with $\tau_i^{(m)} = \tau$ for $i = 1, \dots, n_m$, $m = 2$, $d = 2$. Note that $\mathbf{u}_{i(t+1)}' \mathbf{v}_{j(t+1)} - \mathbf{u}_{it}' \mathbf{v}_{jt} = \mathbf{u}_{i(t+1)}' D\mathbf{v}_{jt} + D\mathbf{u}_{it}' \mathbf{v}_{jt}$. Given the fact that $D\mathbf{u}_{it}$ and $D\mathbf{v}_{jt}$ are assigned with group-wise shrinkage priors, one can consider the distribution of the difference conditional on $\mathbf{u}_{i(t+1)}, \mathbf{v}_{jt}$ as a weighted sum of some shrinkage priors. The summation and integration with \mathbf{u}, \mathbf{v} slightly decrease the mass assigned near the origin by the shrinkage prior. Therefore, adjusting the global scale τ to a smaller value to better accommodate the sparsity structure is necessary. Figure 2 compares the shape of the FFS prior for different τ with the horseshoe prior on components of $D\mathcal{M}_t$ with $\tau = 1$. According to the figure, the shrinkage effect towards $D\mathcal{M}_t$ is much smaller than if we applied the ordinary shrinkage prior to $D\mathcal{M}_t$ with the same τ . We can, however, resolve this problem by using a smaller enough τ . With $\tau = 0.05$, the mass around zero is almost the same as that of a shrinkage prior applied directly to $D\mathcal{M}_t$ with $\tau = 1$, while $\tau = 0.01$ has even more mass around zero. Therefore, FFS priors can achieve a similar component-wise fusion shrinkage on mean matrices if the global prior on τ has a sufficient mass around zero, as described in Assumption 3 in Section 3.

2.2 Posterior post-processing

Due to the continuous nature of shrinkage priors, it is common to perform a post-processing to make further statistical inferences (e.g., variable selection (Hahn and Carvalho, 2015; Bashir et al., 2019) and rank estimation (Chakraborty et al., 2020)). As part of our analysis, we consider two post-processing tasks after obtaining estimates of latent factors: dynamic

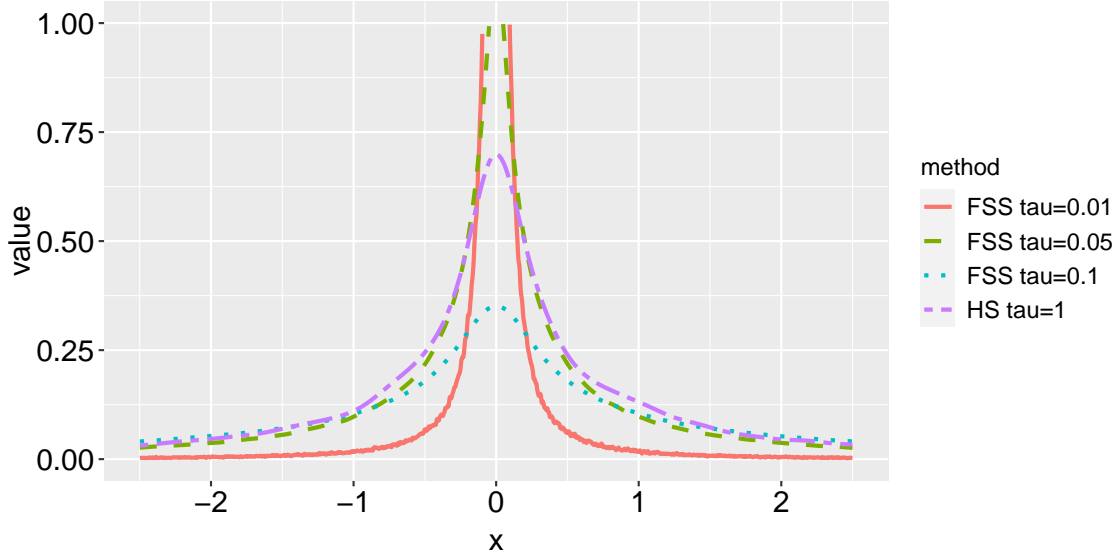


Figure 2: *Density plot Comparisons among marginal priors of $\mathbf{u}'_{i(t+1)}\mathbf{v}_{j(t+1)} - \mathbf{u}'_{it}\mathbf{v}_{jt}$ with different global parameters τ for FFS priors to the horseshoe prior (HS) component-wisely on DM_t with global parameter fixed at $\tau = 1$. Value: values of fitted densities; x : $\mathbf{u}'_{i(t+1)}\mathbf{v}_{j(t+1)} - \mathbf{u}'_{it}\mathbf{v}_{jt}$. Small choices of τ in FFS priors can lead to similar marginal distributions with HS prior applied directly to the component-wise differences.*

comparisons of latent factors and clustering within single time points. For simplicity, the mode index (m) is omitted throughout the subsection.

For dynamic comparisons of latent factors, we consider both adjacent and long-term comparisons, depending on whether the maximal time range compared varies with the number of nodes and time points. Adjacent comparison is commonly used in visualization and change point detection, as it tends to identify the sequence linking latent vectors of subjects from one time to the next. Long-range properties are not commonly considered in dynamic network models but are commonly considered in time series regressions (Robinson, 2003; Palma, 2007), dynamic factor models (Gonzalo and Granger, 1995) and deep neural networks (Hochreiter and Schmidhuber, 1997). In this paper, we handle both adjacent and, firstly, long-range comparisons in the same framework by considering the time range of comparison as a variable k . Consider, for example, when aggregating the information of the estimators $\hat{\mathbf{U}}_{t+1}, \dots, \hat{\mathbf{U}}_{t+k}$ in order to compare the latent vectors among time $t+1, \dots, t+k$, one inherent difficulty is that the row-wise cluster structure of the truth $[\mathbf{U}_{t+1}^{*'}, \dots, \mathbf{U}_{t+k}^{*'}]'$ is destroyed if different orthogonal transformations are applied: the identity rows in $[\mathbf{U}_{t+1}^{*'}, \dots, \mathbf{U}_{t+k}^{*'}]'$ may not be the same anymore in $[(\mathbf{U}_{t+1}^* \mathbf{O}_{t+1})', \dots, (\mathbf{U}_{t+k}^* \mathbf{O}_{t+k})']'$ for different orthonormal matrices $\mathbf{O}_{t+1}, \dots, \mathbf{O}_{t+k}$. In

order to achieve the best possible comparison, Procrustes rotations are the most commonly used approaches (Sarkar and Moore, 2005; Afmann et al., 2016; Papastamoulis and Ntzoufras, 2022). In particular, we adopted the following sequential Procrustes rotations:

$$\hat{\mathbf{O}}_{t(t-1)} = \operatorname{argmin}_{\mathbf{O} \in \mathbb{O}^{d \times d}} \|\hat{\mathbf{U}}_{t-1} \hat{\mathbf{O}}_{(t-1)(t-2)} - \hat{\mathbf{U}}_t \mathbf{O}\|_F, \quad t = 2, \dots, T, \quad (5)$$

with $\mathbf{O}_{10} = \mathbf{I}$ and define the final estimator of latent vectors as $\hat{\mathbf{U}}_1^o = \hat{\mathbf{U}}_1$, $\hat{\mathbf{U}}_2^o = \hat{\mathbf{U}}_2 \hat{\mathbf{O}}_{21}, \dots, \hat{\mathbf{U}}_T^o = \hat{\mathbf{U}}_T \hat{\mathbf{O}}_{T(T-1)}$. Since the latent vectors are projected to the closest one to their previous time points, comparing the current vectors to those before rotations is more reasonable. We then consider the evaluation of the transformed estimated latent vectors across time with a *common* orthogonal transformation of the truth $\mathbf{U}_{t+1}^* \dots \mathbf{U}_{t+k}^*$. A novel loss function to evaluate the simultaneous estimation error of the truth given the estimator $\hat{\mathbf{U}}_{t+1}^o, \dots, \hat{\mathbf{U}}_{t+k}^o$ is then defined as

$$\inf_{\mathbf{O} \in \mathbb{O}^{d \times d}} \sum_{k=1}^k \|\hat{\mathbf{U}}_{t+k}^o - \mathbf{U}_{t+k}^* \mathbf{O}\|_F^2. \quad (6)$$

Therefore, with the consistency under the above loss function (6), the estimator pair after rotations $\hat{\mathbf{U}}_{t+1}^o, \dots, \hat{\mathbf{U}}_{t+k}^o$ could enjoy the same sparse transition property with the truth as the common orthogonal transformation preserves the identity rows in $[\mathbf{U}_{t+1}^{*'} \dots \mathbf{U}_{t+k}^{*'}]'$.

On the other hand, a clustering analysis assigns labels to the subjects $i = 1, \dots, n$, allowing the subjects to be automatically grouped given a time point t . In this article, we obtain such cluster assignment through K_t -means after estimating the latent vectors, similar to spectral clustering, in which K means are obtained after obtaining latent vectors via spectral decomposition (Ng et al., 2001). Assume that the true latent vectors have only K_t distinct rows. Then given any obtained $\hat{\mathbf{U}}$, we can perform a K_t -means analysis on the row vectors of $\hat{\mathbf{U}}_t$:

$$(\hat{\Xi}_t, \hat{\mathbf{U}}_t) = \operatorname{argmin}_{\Xi \in \mathbb{M}_{n, K_t}, \mathbf{X} \in \mathbb{R}^{K_t \times d}} \|\Xi \mathbf{X} - \hat{\mathbf{U}}_t\|_F^2,$$

where \mathbb{M}_{n, K_t} is the collection of membership matrix, whose each row has exactly one 1 and $K_t - 1$ zeros. Then the membership matrix $\hat{\Xi}_t$ reveals the cluster assignments of subjects $i = 1, \dots, n$ at time t . Some variants of K_t -means can also be applied instead, like performing K_t -means after normalizing all the row vectors (Von Luxburg, 2007). There is a strong relationship between K_t -means performance and the separation between the distinct row vectors of $\hat{\mathbf{U}}_t$. As shown in Theorem 3.4, the separation effect of FFS priors plays an important role in encouraging more separate clusters.

3 Theoretical Analysis

In this section, we provide theoretical support for the proposed methodology. We only consider theoretical results for the matrix case, with both matrix factorization and latent space

models. The tensor case should be directly extendable when the number of modes is fixed. We first identify a suitable parameter space (7) (sparse structure in the transitions) for the decomposed low-rank matrices and obtain, in Theorem 3.1, an information-theoretic lower bound on the rate of recovery of $\mathcal{M} = \{\mathbf{M}_t\}_t$ given the parameter space. Then we show in Theorem 3.2 that the rate of contraction of the fractional posterior, a variant of the ordinary posterior (see subsection 3.2), matches the lower bound with only a logarithmic factor, indicating that the fractional posterior mean a nearly rate-optimal estimator. Finally, we provide theoretical results for the post-processing, using dynamic network models as an example in Corollary 3.3 and Theorem 3.4.

For the notation simplicity, we use \mathbf{U}, \mathbf{V} to denote $\mathbf{U}^{(1)}$ and $\mathbf{U}^{(2)}$ respectively. Denote $\Theta = [\mathcal{U}', \mathcal{V}']', \mathcal{U} = [\mathbf{U}_1, \dots, \mathbf{U}_T], \mathcal{V} = [\mathbf{V}_1, \dots, \mathbf{V}_T], \Theta_t = [\mathbf{U}_t', \mathbf{V}_t']'$ and $\boldsymbol{\theta}_{it} = \mathbf{u}_{it}$ if $i = 1, \dots, n$; $\boldsymbol{\theta}_{it} = \mathbf{v}_{(i-n)t}$ if $i = n+1, \dots, n+p$. Let $\boldsymbol{\theta}_{i\cdot} = [\boldsymbol{\theta}'_{i1}, \dots, \boldsymbol{\theta}'_{iT}]'$. Without ambiguity, we use the symbol $\Theta, \Theta_t, \boldsymbol{\theta}_{it}, \boldsymbol{\theta}_{i\cdot}$ for the symmetry case interchangeably with $\mathcal{U}, \mathbf{U}_t, \mathbf{u}_{it}, \mathbf{u}_i$ as well. For a vector \mathbf{x} , we use $\|\mathbf{x}\|_2, \|\mathbf{x}\|_1, \|\mathbf{x}\|_\infty$ represent its ℓ_2, ℓ_1 and ℓ_∞ norms and \mathbf{x}' as its transpose. For a matrix $\mathbf{A} = [\mathbf{a}'_1, \dots, \mathbf{a}'_n]'$, let $\|\mathbf{A}\|_F$ be its Frobenius norm. Given sequences a_n and b_n , we denote $a_n = O(b_n)$ or $a_n \lesssim b_n$ if there exists a constant $C > 0$ such that $a_n \leq Cb_n$ for all large enough n . Similarly, we define $a_n = \Omega(b_n)$ or $a_n \gtrsim b_n$. In addition, let $a_n = o(b_n), a_n = \omega(b_n)$ to be $\lim_{n \rightarrow \infty} a_n/b_n = 0$ or $\lim_{n \rightarrow \infty} b_n/a_n = 0$ respectively.

3.1 Lower bound to the minimax risk

We first consider the following parameter space:

Double-sided Fusion (DSF):

$$\text{DSF}(s_u, s_v) := \left\{ \Theta^* : \sum_{t=2}^T \sum_{i=1}^n \mathbb{1}\{D\mathbf{u}_{it}^* \neq \mathbf{0}\} \leq s_u, \sum_{t=2}^T \sum_{j=1}^p \mathbb{1}\{D\mathbf{v}_{jt}^* \neq \mathbf{0}\} \leq s_v \right. \\ \left. \max_{i=1}^n \max_{t=1}^T \|\mathbf{u}_{it}\|_2 \lesssim 1, \max_{j=1}^p \max_{t=1}^T \|\mathbf{v}_{jt}\|_2 \lesssim 1 \right\}. \quad (7)$$

Due to the above constraint, it is implied that for the total $n \times (T-1)$ transitions of the subjects of \mathbf{U} and $p \times (T-1)$ transitions of the subjects of \mathbf{V} , only s_u and s_v respectively are nonzero transitions, while the rest cases represent the latent vectors remaining unchanged. In addition, under the above boundness assumption, for the Bernoulli likelihood, all the probabilities induced by the inner product $p_{u_{it}^*, v_{jt}^*} := 1/\{1 + \exp(-\mathbf{u}_{it}^{*'} \mathbf{v}_{jt}^*)\}$ are bounded away from 0 and 1. Sparsity level s_u, s_v can be expressed as functions of n, T and p, T . The sparsity constraint above is constructed in a general manner. As a next step, we propose some regularity conditions.

Assumption 1 (KL divergence regularity). *For any $\Theta^a, \Theta^b \in DSF(s_u, s_v)$, we assume the likelihood induced by Θ_t^a, Θ_t^b for all $t = 1, \dots, T$ satisfies:*

$$\max \left\{ D_{KL}(p_{\Theta_t^a}, p_{\Theta_t^b}), V_2(p_{\Theta_t^a}, p_{\Theta_t^b}) \right\} \lesssim \|U_t^a V_t^{a'} - U_t^b V_t^{b'}\|_F^2,$$

where $D_{KL}(p_{\Theta_t^a}, p_{\Theta_t^b})$ is the Kullback–Leibler (KL) divergence and $V_2(p_{\Theta_t^a}, p_{\Theta_t^b}) = \int p_{\Theta_t^a} \{\log(p_{\Theta_t^a}/p_{\Theta_t^b})^2\} dp_{\Theta_t^a}$ is the second order moment of log-likelihood ratio between $p_{\Theta_t^a}$ and $p_{\Theta_t^b}$.

The assumption holds for many commonly used likelihood functions, like Gaussian and binary with true probabilities bounded away from 0 and 1. Given an estimator $\hat{\Theta}$ of Θ^* , we consider the squared loss

$$\frac{1}{npT} \sum_{t=1}^T \|\hat{U}_t \hat{V}_t' - U_t^* V_t^{*'}\|_F^2$$

to formulate the minimax lower bound. Since U_t, V_t can only be identified up to rotation and scaling, the loss function is formulated in terms of the matrix products, which are rotation and scaling invariants. Then the following statement holds for the minimax lower bound:

Theorem 3.1. *Suppose the data generating process follows equation (4) and Assumption 1 holds, then suppose that d is fixed. For large enough n, p, T , we have:*

$$\begin{aligned} & \inf_{\hat{\Theta}} \sup_{\Theta \in DSF(s_u, s_v)} \mathbf{E}_{\Theta} \left[\frac{1}{Tnp} \sum_{t=1}^T \|\hat{U}_t \hat{V}_t' - U_t^* V_t^{*'}\|_F^2 \right] \\ & \gtrsim \frac{1}{npT} \left\{ s_u \log \left(\frac{Tn}{s_u} \right) + s_v \log \left(\frac{Tp}{s_v} \right) + n + p \right\}. \end{aligned}$$

As far as we know, there is no similar result in the literature to Theorem 3.1 concerning the estimation of low-rank structured fused matrices with an information-theoretic lower bound. Note that we ignore the latent dimension d explicitly in the bound by assuming it is a fixed constant across time. $s_u \log(Tn/s_u)/(npT)$ and $s_v \log(Tp/s_v)/(npT)$ are the selection errors for the fusion structure of \mathcal{U} and \mathcal{V} respectively. $(n+p)/(npT)$ identifies the initial estimation errors: even in the extreme case that $s_u = s_v = 0$, where all matrices are equal, it is still necessary to estimate U_1 and V_1 . This matches the minimax lower bound $1 + s \log(T/s)$ of the linear fused model (Fan and Guan, 2018) with fusion sparsity s . On the other hand, in the dense case where $s_u \geq cnT, s_v \geq cpT$ for some constant $c > 0$, the lower bound is then $(n+p)/(np)$, which equates to estimating each low-rank mean matrix individually. If n and p are approximately equal, then both \mathcal{U} and \mathcal{V} need to be structurally fused to deliver a measurable improvement in the lower bound. However, in the case of only a one-sided fusion structure, the lower bound may not even be improved from the error rate of the static case $(n+p)/(np)$.

3.2 Posterior contraction rate under FFS priors

In order to facilitate the theoretical analysis of the proposed model, we adopt the fractional posterior (Walker and Hjort, 2001) framework, where the usual likelihood $P(\mathcal{Y} \mid \mathcal{U}, \beta)$ is raised to a power $\alpha \in (0, 1)$ to form a pseudo-likelihood $P_\alpha(\mathcal{Y} \mid \mathcal{U}, \beta) := [P(\mathcal{Y} \mid \mathcal{U}, \beta)]^\alpha$, leading to a fractional posterior $P_\alpha(\mathcal{U}, \beta \mid \mathcal{Y}) \propto P_\alpha(\mathcal{Y} \mid \mathcal{U}, \beta) p(\mathcal{U}) p(\beta)$. Such adaptation only requires minor changes in computation, while the theoretical analysis requires fewer conditions than the usual posterior (Bhattacharya et al., 2019). Similarly to the original posterior, the optimal convergence of a fractional posterior can imply a rate-optimal point estimator derived from the fractional posterior. We then need the following assumptions to establish results for the posterior convergence:

Assumption 2 (Likelihood regularity). *For any $0 < \alpha < 1$, and $\Theta^a, \Theta^b \in DSF(s_u, s_v)$, the α -divergence induced by Θ^a, Θ^b for all $t = 1, \dots, T$ satisfies:*

$$D_\alpha(p_{\Theta^a}, p_{\Theta^b}) \gtrsim \|\mathbf{U}_t^a \mathbf{V}_t^{a'} - \mathbf{U}_t^b \mathbf{V}_t^{b'}\|_F^2.$$

Assumption 3 (Global prior). *For any $s_i = 1, \dots, \max\{n, p\}$, with $\log T = o(np)$, the global prior g satisfies:*

$$\log \{g(\tau_i^* < \tau < 2\tau_i^*)\} \gtrsim -s_i \log(npT), \quad \text{with} \quad \tau_i^* = \frac{s_i^{\frac{1}{2}} (\log(npT))^{\frac{1}{2}}}{(np)^{\frac{3}{2}} T^{\frac{5}{2}}}.$$

Similar to Assumption 1, Assumption 2 also holds for Gaussian and binary cases with true probabilities bounded away from 0 and 1, see Gil et al. (2013) for some detailed calculations. Assumption 3 requires that the global prior has sufficient mass around proper small values, it can be satisfied by the priors $\tau \sim \text{Ca}^+(0, 1)$ or $\tau^2 \sim \text{Gamma}(a_\tau, b_\tau)$ with constants a_τ, b_τ as shown in the appendix. Then we have the following main theorem:

Theorem 3.2. *Suppose the data generating process follows equation (4) and Assumptions 1, 2 and 3 hold. Then under the prior (3), if $\Theta^* \in DSF(s_u, s_v)$ with $\log T = o(np)$ and d is fixed. Denote $\epsilon_{n,p,T} = M \sqrt{(s_u + s_v + n + p) \log(npT) / npT}$ for some constant $M > 0$. Then for large enough n, p, T , any $D \geq 2$ and $\eta > 0$, with probability at least $1 - 2/\{(D - 1 + \eta)^2 npT \epsilon_{n,p,T}^2\}$, we have*

$$\Pi_\alpha \left\{ \frac{1}{Tnp} \sum_{t=1}^T \|\mathbf{U}_t \mathbf{V}_t' - \mathbf{U}_t^* \mathbf{V}_t^{*'}\|_F^2 \geq \frac{D + 3\eta}{1 - \alpha} \epsilon_{n,p,T}^2 \mid \mathcal{Y} \right\} \leq e^{-\eta npT \epsilon_{n,p,T}^2}.$$

The above theorem indicates that the fractional posterior of the average estimation error can achieve the minimax lower bound with only a logarithm factor when the true lists of row vectors of \mathcal{U} and \mathcal{V} are both group-wise fused. In the worst case, such a fusion type of lower bound can not be matched by ℓ_1 penalized regressions (Fan and Guan, 2018). Therefore, theoretically, the proposed method is better than the related literature that uses

ℓ_1 regularization to introduce a fusion structure. The proof of Theorem 3.2 is based on an ℓ_1 type of prior concentration for the shrinkage prior shown in the supplementary material. The above theorem also demonstrates an advantage in comparison of the conditions required with the fusion model with only one variable: when there is only one variable of time T with fusion sparsity s , then $s = o(T/\log(T))$ is required to make sure that the targeted rate $s \log T/T$ could converge to zero; however, while the fusion structure holds for np variables, with the error rate $s_i \log(npT)/(npT) = s_i \log(np)/(npT) + s_i \log(T)/(npT)$ for a subject with sparsity s_i . As long as a mild assumption $\log T = o(np)$ holds, the above rate converges to zero even if $s_i = T$, which is considerably more flexible since the successive differences of some subjects are therefore permitted to be non-sparse. The above conclusion matches the aggregation form of the constraints in equation (4), which is more relaxed than requiring that all successive differences are simultaneously group-wise sparse.

In the next subsection, we use dynamic network models as an example to show the theoretical results for the post-processing as described in Section 2.2 after obtaining the estimates.

3.3 Theoretical results for post-processing under dynamic network models

For dynamic network models, the estimation error in the inner product in Theorem 3.2 cannot directly imply the best recovery of latent vectors for the purposes of dynamic comparison. To handle the issue, we study the recovery of latent vectors in the loss function (6). In particular, we divide the time $1, \dots, T$ to T/k sets, where each set contains k consecutive time points: $\{(t-1)k+1, \dots, (t-1)k+k\}_{t=1}^{T/k}$. We assume $\bar{t} = T/k$ is an integer for simplicity. We consider the comparison for latent space within each set of time period so that the maximal time gap is k for each comparison. Then the following corollary characterizes the optimal estimation error of the estimator after sequential Procrustes rotations (5):

Corollary 3.3. *Suppose the Assumptions in Theorem 3.2 hold. In addition, assume that the smallest singular of \mathbf{U}_t^* , denoted as λ_t , satisfies $\lambda_t = \Omega(\sqrt{n})$ for $t = 1, \dots, T$. For the posterior means estimated $\hat{\mathbf{U}}_t$, after performing sequential Procrustes rotations (5) to obtain estimation $\hat{\mathbf{U}}_1^o, \dots, \hat{\mathbf{U}}_T^o$, the average error for all windows satisfies*

$$\begin{aligned} \frac{1}{nT} \sum_{t=1}^{\bar{t}} \inf_{\bar{\mathbf{O}}_{t,k} \in \mathbb{O}^{d \times d}} \sum_{k_0=1}^k \|\hat{\mathbf{U}}_{(t-1)k+k_0}^o - \mathbf{U}_{(t-1)k+k_0}^* \bar{\mathbf{O}}_{t,k}\|_F^2 &\lesssim \frac{(s+n) \log(nT)}{n^2 T} \\ &+ \min \left\{ \frac{k(s+n) \log(nT)}{n^2 T}, \frac{\log(nT)}{n} \right\} + \min \left\{ \frac{sk(k-1)}{nT}, \frac{s}{n}, 1 \right\}. \end{aligned}$$

There is an additional assumption characterizing the lower bound of the order of the smallest eigenvalue of the true latent vectors. The lower bound of the order \sqrt{n} holds for many matrices: for example, for an $n \times d$ random matrix whose entries are i.i.d. distributed

with zero mean and unit variance, the famous Bai-Yin's law (Bai and Yin, 2008) states that its smallest singular value is approximately $\sqrt{n} - \sqrt{d}$ (we refer Vershynin (2010) for more matrices with the same rate). When $k = 1$, the error rate becomes the optimal estimation error in Theorem 3.2. When k is a constant where the comparison is limited to adjacent ones, the average error for all windows converge to zero at rate $(s + n) \log(nT)/(n^2T) + s/(nT)$ as $n, T \rightarrow \infty$, leading to consistency as long as $s = o(nT)$. If the transition is extremely sparse $s = o(n)$, then one can simultaneously compare all the latent space for all time points of length $k = O(T)$. For the challenging case, where $s = o(nT)$, only constant time latent positions can be compared across time. In some special cases, the above error rate is not optimal. We provide in supplement subsection 7.8 of an improvement under a more stringent assumption of the true transitions. To our best knowledge, although Procrustes rotations have been popularly employed, there is no similar theoretical result to Corollary 3.3 that tries to quantitatively understand the possibility and limitations of long-term comparison of the estimated latent factors, which discusses long-term properties of dynamic networks from a theoretical aspect.

Once the latent vectors have been obtained, K -means can be used to cluster the subjects. This is equivalent to detecting communities within networks. For any membership matrix Ξ , the cluster membership of a subject i is denoted by $g_i \in \{1, \dots, K\}$, which satisfies $\Xi i g_i = 1$. Let $G_k(\Xi) = \{1 \leq i \leq n : g_i = k\}$. We consider the following loss function to evaluate clustering accuracy

$$L(\hat{\Xi}, \Xi) = \min_{\mathbf{J} \in E_K} \|\hat{\Xi} \mathbf{J} - \Xi\|_{2,0},$$

which represents the number of misclustering subjects, where E_K is the set of all $K \times K$ permutation matrix.

Our next result concerns performing separate community detection for each network while improving the overall misclustering rate based on the network dependence structure.

Theorem 3.4. *Suppose the assumptions in Theorem 3.2 hold. In addition, assume that for $t = 1, \dots, T$, the truth \mathbf{U}_t^* satisfies:*

1. \mathbf{U}_t^* has K_t distinct rows: $\mathbf{U}_t^* = \Xi_t^* \mathbf{X}_t$, $\Xi_t^* \in \mathbb{M}_{n, K_t}$ for some $K_t > 0$ and $\mathbf{U}_t^* \in \mathbb{R}^{K_t \times d}$ is full rank;
2. The smallest singular value of \mathbf{U}_t^* , denoted as λ_t , satisfies $\lambda_t = \Omega(\sqrt{n})$;
3. Cluster separation: $\delta \leq \min_{i \neq j} \|\mathbf{u}_{it}^* - \mathbf{u}_{jt}^*\|_2$ for any $\mathbf{u}_{it}^* \neq \mathbf{u}_{jt}^*$, where $\delta > 0$;
4. The minimal block size satisfies $\min_i |G_i(\Xi_t^*)| = \omega(\log(n)/\delta^2)$.

Then after performing K_t -means for posterior means $\hat{\mathbf{U}}_t$ to obtain estimation of membership matrix $\hat{\Xi}_t$, as $n, T \rightarrow \infty$, we have

$$\frac{1}{T} \sum_{t=1}^T L(\hat{\Xi}_t, \Xi_t^*) \lesssim \frac{(s + n) \log(nT)}{nT\delta^2}.$$

There exists a list of literature discussing community detection given a list of time-dependent networks under different settings (Liu et al., 2018; Pensky and Zhang, 2019). Assumption 1 is prevalent in the literature on community detection for networks. Assumption 3 represents a minimum separation between different clusters, which can be a constant for many cases: For example, $\delta = 1$ for a random matrix whose entries are i.i.d. binary distributed. Assumption 4 requires a minimum block size of the clusters. The usage of shrinkage prior is justified by the cluster separation. Suppose at time t we have $\mathbf{u}_{it}^* = \mathbf{u}_{jt}^*$ for subjects i, j . Then for time $t + 1$, the subject i move to another cluster while subject j stay the same. Under the cluster separation condition, we have $\delta_{t+1} \leq \|\mathbf{u}_{j(t+1)}^* - \mathbf{u}_{i(t+1)}^*\|_2 = \|\mathbf{u}_{j(t+1)}^* - \mathbf{u}_{jt}^*\|_2$, which requires the transitions of the subjects to be heterogeneous: either the transition is zero, or the transition is large. However, when nonparametric priors (e.g., Gaussian process priors) are adopted on the transitions, one assumes that the true difference satisfies some smoothness condition, which cannot adapt to the above heterogeneous requirement.

Although we only offer post-processing for network models, such a framework can also be applied to matrix factorization and tensor models if not only the inner product but also the latent factors can be recovered up to orthogonal transformations; see Yu et al. (2020) for an example.

4 Computation

From a computational perspective, while sampling-based posterior computation is not difficult to design, to accelerate the computation with a large number of parameters, variational inference is used as the computation strategy to provide an estimate. With variational inference, we aim to approximate the fractional posterior $p_\alpha(\mathcal{U}, \beta \mid \mathcal{Y})$ defined in subsection 3.2 by finding the closest member of the family of distributions Γ to the posterior. Due to the temporal dependence and simultaneously shrinkage of the model, we may consider the following structured mean-field variational (SMF) family Γ :

$$q(\mathcal{U}, \beta) = \prod_{m=1}^M \prod_{i=1}^n q(\mathbf{u}_i^{(m)}) q(\beta), \quad (8)$$

where $\mathbf{u}_i^{(m)} = [\mathbf{u}_{i1}^{(m)'}, \dots, \mathbf{u}_{iT}^{(m)'}]'$. The adopted SMF family accommodates the special structures of the $Td \times Td$ covariance matrix for $\mathbf{u}_i^{(m)}$, which includes the temporal dependence across time $t = 1, \dots, T$ and the group-wise dependence among components for the same subject i . Note that the covariance of $\mathbf{u}_i^{(m)}$ is in a block tri-diagonal structure, which only requires $O(Td^3)$ operations to invert via the Kalman smoothing framework (Kalman, 1960). We begin by examining the simpler matrix case (4), and then extend the algorithm to the general tensor case (1).

4.1 Matrix-valued data

The goal of variational inference is

$$\hat{q}(\Theta, \beta) = \underset{q(\Theta, \beta) \in \Gamma}{\operatorname{argmin}} D_{KL} \{q(\Theta, \beta) \parallel p_\alpha(\Theta, \beta \mid \mathcal{Y})\} = \underset{q(\Theta, \beta) \in \Gamma}{\operatorname{argmin}} -\mathbf{E}_q \left\{ \log \left(\frac{p_\alpha(\mathcal{Y}, \Theta, \beta)}{q(\Theta, \beta)} \right) \right\},$$

where the term $\mathbf{E}_q \{\log(p_\alpha(\mathcal{Y}, \Theta, \beta)/q(\Theta, \beta))\}$ is the evidence-lower bound (ELBO) and $p_\alpha(\Theta, \beta \mid \mathcal{Y})$ is the marginal posterior $p_\alpha(\Theta, \beta \mid \mathcal{Y}) = \int p_\alpha(\Theta, \beta, \mathbf{\Lambda}, \boldsymbol{\sigma}_0 \mid \mathcal{Y}) d\mathbf{\Lambda} d\boldsymbol{\sigma}_0$. Recall that we denote $\Theta = [\mathcal{U}', \mathcal{V}']'$, $\boldsymbol{\Theta}_t = [\mathbf{U}'_t, \mathbf{V}'_t]'$ and $\boldsymbol{\theta}_{it} = \mathbf{u}_{it}$ if $i = 1, \dots, n$; $\boldsymbol{\theta}_{it} = \mathbf{v}_{(i-n)t}$ if $i = n+1, \dots, n+p$ for notation simplicity.

The variational posterior under given SMF (8) can be obtained through coordinate ascent variational inference algorithm (CAVI) to maximize the ELBO (Blei et al. (2017)):

$$q^{(new)}(\beta) \propto \exp[\mathbf{E}_{-\beta} \{\log P(\Theta, \beta, \mathcal{Y})\}]; \quad q^{(new)}(\boldsymbol{\theta}_{i\cdot}) \propto \exp[\mathbf{E}_{-\boldsymbol{\theta}_{i\cdot}} \{\log P(\Theta, \beta, \mathcal{Y})\}], \quad (9)$$

where $\mathbf{E}_{-\beta}$, $\mathbf{E}_{-\boldsymbol{\theta}_{i\cdot}}$ are the expectations taken with respect to density $\prod_{i=1}^n q(\boldsymbol{\theta}_{i\cdot})$ and $\prod_{i=1}^n \prod_{j \neq i} q(\boldsymbol{\theta}_{j\cdot}) q(\beta)$.

Nevertheless, minimization of the above KL divergence towards the marginal posterior $p_\alpha(\Theta, \beta \mid \mathcal{Y})$ (after marginalizing $\boldsymbol{\sigma}_0 = \{\sigma_{0i}\}$, $\boldsymbol{\tau} = \{\tau_i\}$, $\mathbf{\Lambda} = \{\lambda_{it}\}$) cannot yield efficient closed-form updating formulas and must be done by either integrating or Monte Carlo approximations. Instead, we consider minimizing the KL divergence towards the joint posterior as the surrogate. Furthermore, we adopt the variable augmentation that the square of the half-Cauchy distribution can be expressed as a mixture of Inverse-Gamma distributions (Neville et al., 2014): for $\lambda_{it} \sim \text{Ca}^+(0, 1)$, we can write

$$\lambda_{it}^2 \mid \eta_{it} \sim \text{IG}\left(\frac{1}{2}, \frac{1}{\nu_{it}}\right), \quad \eta_{it} \sim \text{IG}\left(\frac{1}{2}, 1\right).$$

Denote $\mathbf{H} = \{\eta_{it}\}_{i,t}$. Then the objective of the KL minimization is as follows:

$$\hat{q}(\Theta, \beta, \mathbf{H}, \mathbf{\Lambda}, \boldsymbol{\tau}, \boldsymbol{\sigma}_0) = \underset{q(\Theta, \beta, \mathbf{H}, \mathbf{\Lambda}, \boldsymbol{\tau}, \boldsymbol{\sigma}_0) \in \Gamma}{\operatorname{argmin}} -\mathbf{E}_q \left\{ \log \left(\frac{p_\alpha(\mathcal{Y}, \Theta, \beta, \mathbf{H}, \mathbf{\Lambda}, \boldsymbol{\tau}, \boldsymbol{\sigma}_0)}{q(\Theta, \beta, \mathbf{H}, \mathbf{\Lambda}, \boldsymbol{\tau}, \boldsymbol{\sigma}_0)} \right) \right\},$$

where now the SMF family is defined as:

$$q(\Theta, \beta, \mathbf{H}, \mathbf{\Lambda}, \boldsymbol{\tau}, \boldsymbol{\sigma}_0) = \prod_{i=1}^{n+p} \left[q(\boldsymbol{\theta}_{i\cdot}) q(\tau_i) \prod_{t=1}^{T-1} \{q(\lambda_{it}) q(\eta_{it})\} q(\sigma_{0i}) \right] q(\beta). \quad (10)$$

Given the above variational family (10), $q(\eta_{it})$, $q(\lambda_{it}^2)$ and $q(\sigma_{0i}^2)$ can be updated in inverse-Gamma conjugate family. Moreover, updates of $q(\boldsymbol{\tau})$ can also have a closed-form expression if the recommended half-Cauchy prior or Gamma prior is used. In addition, the updating of $q(\beta)$ and $q(\boldsymbol{\theta}_{i\cdot})$ can be efficiently obtained through a message-passing framework when the likelihood is either Gaussian or Bernoulli. For completeness, we

provide all the above derivations in the supplementary material Section 7.12. While CAVI algorithms are applied to models with sparsity structures, the final accuracy is highly sensitive to the order of component-wise updating: As noted in Huang et al. (2016), errors can accumulate when updating is done in a naive cyclical manner; Ray and Szabó (2021) proposed a prioritized updating approach for sparse regression in order to prevent this. In our algorithm, we partition the subject-related components into different blocks based on the index of the subject $\{q(\boldsymbol{\theta}_{i\cdot}), q(\sigma_{0i}), q(\boldsymbol{\lambda}_{i\cdot}), q(\tau_i), q(\boldsymbol{\eta}_{i\cdot})\}_{i=1,\dots,n+p}$, in order to avoid error accumulation. Then we update them block-by-block: we update components in the i th block $\{q(\boldsymbol{\theta}_{i\cdot}), q(\sigma_{0i}), q(\boldsymbol{\lambda}_{i\cdot}), q(\tau_i), q(\boldsymbol{\eta}_{i\cdot})\}$ until convergence (the gap between prediction errors in two consecutive steps is small enough), and then move onto the next block. In contrast to the cyclic updating of all components, the block-wise updating strategy can reduce the cumulative error when updating a new block. Each block's convergence is fast because the variational family (10) captures the temporal dependence. We compare the algorithm for each block with the proximal gradient descent with an ℓ_1 penalized objective function in section 7.4 in the supplement.

4.2 Tensor Data

For tensor data, the shrinkage priors are similarly applied on the transitions $\mathbf{u}_{it}^{(m)} \mid \mathbf{u}_{i(t-1)}^{(m)} \sim \mathcal{N}(\mathbf{u}_{i(t-1)}^{(m)}, \tau_i^{(m)2} \lambda_{it}^{(m)2})$, and the SMF family is similarly defined:

$$q(\mathcal{U}, \beta, \mathbf{H}, \boldsymbol{\Lambda}, \boldsymbol{\tau}, \boldsymbol{\sigma}_0) = \prod_{m=1}^m \prod_{i=1}^{n_m} \left[q(\mathbf{u}_{i\cdot}^{(m)}) q(\tau_i^{(m)}) \prod_{t=1}^{T-1} \left\{ q(\lambda_{it}^{(m)}) q(\eta_{it}^{(m)}) \right\} q(\sigma_{0i}^{(m)}) \right] q(\beta).$$

Then the extension from matrix to tensor is based on the tensor unfolding technique, as in Hoff (2011) and Zhou et al. (2013). Tensor unfolding allows the components of the mean to be expressed as inner products of a targeted vector and component-wise products of some other vectors, which is fortunate to be compatible with the alternating updatings of the SMF variational family. Note that when we assume \mathcal{M}_t defined as equation (1), we have the mode- m unfolding:

$$\mathcal{M}_{t,(m)} = \left\{ \mathbf{U}_t^{(M)} \odot \dots \mathbf{U}_t^{(m+1)} \odot \mathbf{U}_t^{(m-1)} \odot \dots \mathbf{U}_t^{(1)} \right\} \mathbf{U}_t^{(m)'} ,$$

where \odot is the Khatri-Rao product: $\mathbf{A} \odot \mathbf{B} = [\mathbf{a}_1 \otimes \mathbf{b}_1, \dots, \mathbf{a}_K \otimes \mathbf{b}_K]$ for $\mathbf{A} = [\mathbf{a}_1, \dots, \mathbf{a}_K] \in \mathbb{R}^{I \times K}$ and $\mathbf{B} = [\mathbf{b}_1, \dots, \mathbf{b}_K] \in \mathbb{R}^{J \times K}$. Therefore, the components of $\mathcal{M}_{t,(m)}$ equal inner products between row vectors of $\mathbf{U}_t^{(M)} \odot \dots \mathbf{U}_t^{(m+1)} \odot \mathbf{U}_t^{(m-1)} \odot \dots \mathbf{U}_t^{(1)}$ and $\mathbf{U}_t^{(m)}$. In particular, for $\{i_m = 1, \dots, n_m\}_m$, we have

$$\left\{ \mathbf{u}_{i_M t}^{(M)} \circ \dots \mathbf{u}_{i_{m+1} t}^{(m+1)} \circ \mathbf{u}_{i_{m-1} t}^{(m-1)} \circ \dots \mathbf{u}_{i_1 t}^{(1)} \right\}' \mathbf{u}_{j t}^{(m)} = [\mathcal{M}_{t,(m)}]_{i,j}$$

with $i = (i_M - 1)(\prod_{j=1, j \neq M}^{M-1} n_j) + \dots + (i_{m+1} - 1)(\prod_{j=1}^{m-1} n_j) + (i_{m-1} - 1)(\prod_{j=1}^{m-2} n_j) + \dots + i_1$, where \circ is the Hadamard (element-wise) product. In the CAVI algorithm for the SMF

family, when all the targeted row vectors follow Gaussian distributions, calculating the first and second moments of $\mathbf{u}_{i_M t}^{(M)} \circ \dots \circ \mathbf{u}_{i_{m+1} t}^{(m+1)} \circ \mathbf{u}_{i_{m-1} t}^{(m-1)} \circ \dots \circ \mathbf{u}_{i_1 t}^{(1)}$ is necessary to update a new mean and covariance for the distribution of $\mathbf{u}_{i_m t}^{(m)}$. For the component-wise product above, the first moment is straightforward, and the following lemma can be used to calculate the second moment sequentially:

Lemma 4.1. *Suppose $\mathbf{a} \sim \mathcal{N}(\boldsymbol{\mu}, \boldsymbol{\Sigma})$ and $\boldsymbol{\Xi}$ is a positive definite matrix. Let $\mathbf{D}(\mathbf{a}) = \text{diag}(\mathbf{a})$, then we have*

$$\mathbf{E}(\mathbf{D}(\mathbf{a})\boldsymbol{\Xi}\mathbf{D}(\mathbf{a})) = \mathbf{D}(\boldsymbol{\mu})\boldsymbol{\Xi}\mathbf{D}(\boldsymbol{\mu}) + \boldsymbol{\Xi} \circ \boldsymbol{\Sigma},$$

With the lemma, given $\mathbf{E}(\mathbf{a}\mathbf{a}')$ and $\mathbf{b} \sim \mathcal{N}(\boldsymbol{\mu}_b, \boldsymbol{\Sigma}_b)$, we can first calculate $\mathbf{E}((\mathbf{b} \circ \mathbf{a})(\mathbf{b} \circ \mathbf{a})') = \mathbf{E}(\mathbf{D}(\mathbf{b})\mathbf{a}\mathbf{a}'\mathbf{D}(\mathbf{b}))$. Then $\mathbf{E}((\mathbf{c} \circ \mathbf{b} \circ \mathbf{a})(\mathbf{c} \circ \mathbf{b} \circ \mathbf{a})')$ can also be calculated sequentially with another normal distributed vector \mathbf{c} . A similar technique can also be applied when additional auxiliary variables are estimated using additional MF factorization. For example, to estimate the variance of the noise of a Gaussian tensor model σ , commonly used inverse-Gamma conjugate updates can be applied together within the MF framework, then the necessary term $\mathbf{E}_q\{\sum_{t=1}^T (\mathcal{Y}_t - \mathcal{M}_t)^2\}$ can also be computed through the above strategy.

5 Data Analysis

5.1 Simulations

In the section, we perform simulations to show that the simultaneous low-rank and fusion structures can not be fully captured by some methods that only consider low-rankness or fusion structures. First, simulation cases are considered to compare with the following approaches:

- SVD1: perform SVD to obtain the best rank d approximation for matrices at each time;
- SVD2: combine the observed matrices at the neighbor time together to perform a low-rank approximation: let $\tilde{\mathbf{Y}}_t = [\mathbf{Y}_{t-1}, \mathbf{Y}_t, \mathbf{Y}_{t+1}]$ ($\tilde{\mathbf{Y}}_1 = [\mathbf{Y}_1, \mathbf{Y}_2]$ and $\tilde{\mathbf{Y}}_T = [\mathbf{Y}_{T-1}, \mathbf{Y}_T]$). We then perform low-rank approximation on $\tilde{\mathbf{Y}}_t$ where the rank is obtained by optimal hard thresholding (Gavish and Donoho, 2014), and the estimator $\hat{\mathbf{Y}}_t$ is the corresponding sub-matrix of the low-rank estimator of $\tilde{\mathbf{Y}}_t$;
- Flasso1: perform fused lasso to estimate each component over time separately;
- Flasso2: perform fused lasso to estimate each component over time separately, then apply SVD to obtain the best rank d approximation for each estimated matrix.
- CP: perform CP decomposition to obtain the best rank d approximation for tensors at each time.

SVD2 and Flasso2 are some modified approaches based on SVD and fused lasso to consider both low-rank and fusion structures in the final estimation, either based on a data argumentation or a two-step approach. Throughout all simulation and real data analyses, we fix the fractional power for the fractional likelihood defined in subsection 3.2 as $\alpha = 0.95$, hyperparameters $a_{\sigma_0} = b_{\sigma_0} = 1/2$. First, 25 replicated data sets are generated from the following case:

Case 1, Gaussian factorization model: $n, p = 5, 10, 20, 50$ with $n \geq p$,

$$\begin{aligned} \mathbf{u}_{i1}^{(m)} &\sim \mathcal{N}(\mathbf{0}, \mathbb{I}), \quad i = 1, \dots, n_m, m = 1, 2, \\ D\mathbf{u}_{it}^{(m)} &= \begin{cases} (0, 0)' & \text{with probability } \rho \\ (-1, -1)' & \text{with probability } (1 - \rho)/2 \\ (1, 1)' & \text{with probability } (1 - \rho)/2, \end{cases} \quad i = 1, \dots, n; t = 2, \dots, T \\ Y_{ijt} &\sim \mathcal{N}(\mathbf{u}_{it}^{(1)'} \mathbf{u}_{jt}^{(2)}, 0.3^2) \quad i = 1, \dots, n_1; j = 1, \dots, n_2; t = 1, \dots, T. \end{aligned}$$

The supplement provides two additional cases about the binary network model and the tensor model in subsection 7.1.1. We have $T = 100$, $d = 2$, $\rho = 0.5, 0.8, 0.85, 0.9, 0.95, 0.99$ across all cases. Note that in the above simulations the expected number of effective parameters is $(n + p)(1 - \rho)Td$ for the Gaussian factorization model, $n^2Td(1 - \rho)$ for the binary network model and $(n_1 + n_2 + n_3)Td(1 - \rho)$ for the tensor model. The piecewise change of binary and tensor cases is small to ensure that the absolute value of all latent vectors is bounded. Simulation settings for FFS are as follows: In the Gaussian case, iterations are stopped when the difference between predictive RMSEs in two consecutive cycles is less than 10^{-4} . The root mean squared error is used to measure the discrepancy between the estimated and true latent distances. We use the sample Pearson's correlation coefficient (PCC) in the binary case to measure the discrepancy between the true and estimated probabilities. The stopping criterion is the difference between the training AUC (area under the curve) in two consecutive cycles not exceeding 0.01. For the fused lasso, we use cross-validation to tune the hyperparameters. Note that all np components are required to perform separately fused lasso with cross-validations. We only perform Flasso1 and Flasso2 in Case 1 because the mean can not be estimated under the logistic link for a binary response without a predictor.

Figure 3 provides some numerical support for our theoretical results in multiple aspects. First, as ρ increases, the estimation errors of FFS, Flasso1, Flasso2 and SVD2 decrease, whereas that of SVD barely changes. The reason is that SVD estimates observation matrices separately without considering temporal dependence, whereas other approaches can take advantage of dynamic dependence in the model. It can be seen that even though SVD2 can take into account partial temporal dependence, the exact fusion structure can not be captured, leading to large estimation errors than the proposed approach. Moreover, by comparing Flasso and Flasso 2, we can see that the simultaneously low-rank and fusion

structure should be considered if the true data generating process is constrained in that way. When the number of observations is sufficient, FFS consistently achieves lower RMSE than all other approaches. The more accurate estimation of FFS over Flasso and Flasso2 matches the theoretical results that our final estimators are near minimax optimal while the ℓ_1 type of regularizations is not.

Finally, we perform simulations in the context of dynamic network models to demonstrate the effectiveness of FFS in dynamic comparison and clustering in the presence of sparse changes. We compare FFS priors to IGLSM, where we implement IGLSM via the same likelihood and variational inference framework, only changing the prior for the transition variance. We adopt the same simulation setting with Figure 1 to compare the dynamic comparisons over a long period, only changing the sample size to $n = 20$. Only nodes 1, 2 transit, and the rest of the nodes stay static over time. First, as illustrated in Figure 4, for IGLSM, the same property from the truth can not be detected. As almost all nodes move across time, it is difficult to identify whether the moving of the node positions is due to random error or the intrinsic property of the truth. However, the property shown in Corollary 3.3 can be used to detect such properties of FFS: Under the proposed FFS prior, the latent positions across time can be compared whenever the majority of the truth remains static over time with $s = o(n)$.

For comparison in clustering, the following setup is considered: Let $d = 2, n = 40, T = 100$. The initial distribution of each component of the true latent vectors is uniformly sampled from $\{-2, 2\}$, so that there are $2^d = 4$ true clusters across all time: $(-2, -2), (-2, 2), (2, -2), (2, 2)$. Next, we select the static subjects with a probability p_1 and do not allow them to change over time. The remaining subjects change with a probability of $1 - p_2$ at each time, uniformly switching to the other 3 locations with a probability of $(1 - p_2)/3$. Thus, the expected number of changes of cluster membership is $nT(1 - p_1)(1 - p_2)$. We generate data according to the model $Y_{ijt} \sim \text{Ber}(\text{logistic}(-2 - \mathbf{u}'_{it}\mathbf{u}_{jt})), i > j; Y_{ijt} = Y_{jit}, t = 1, \dots, T$, where the intercept -2 is to make sure the connection probabilities between cluster $(-2, 2)$ and $(2, -2)$ are small enough. After obtaining the estimate of the latent vectors via variational means, we normalized all the latent subjects, performed Procrustes rotations (5) and then applied K -means with 4 centers at each time independently. Finally, the average rand index over time between the true cluster and the estimated cluster determined by K -means is used to assess the accuracy of the clustering. Simulations are repeated 25 times, and the results are shown in Figure 5. According to the figure, FFS performs no worse than IGLSM when either p_1 or p_2 is large. On the other hand, FFS performs worse than IGLSM when the sparsity assumption is violated, where both p_1 and p_2 are relatively small, for instance, when $p_1 = 0.5, p_2 = 0$ which indicates that the cluster memberships change among 50% of the total $n(T - 1)$ transitions. In general, the more sparse the transitions, the better the performance in clustering, both for FFS and IGLSM, since sparsity introduces more dependence across time. While when the transitions are extreme sparse, both approach perform similarly, see the case $p_1 = 0.9, p_2 = 0.75$. This is because using Procrustes rotations is good enough to capture the temporal dependence when there are almost no changes in

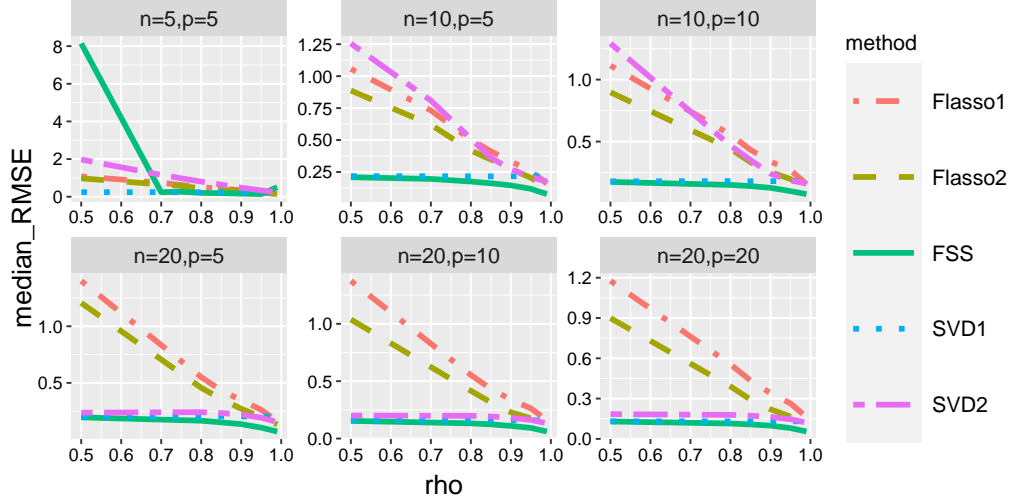


Figure 3: *Performance comparison for Case 1 between FFS, SVD and Flasso. The measure is the median RMSE for the mean estimation of \mathcal{M} across 25 replicates. ρ : ρ , the probability of remaining static for each time point and observation. FFS achieves lower RMSE than all other approaches when the number of observations is sufficient (except in the case $n = 5, p = 5$).*

the true latent vectors. In summary, FFS better captures the dependence introduced by sparsity in transitions than IGLSM.

5.2 Formal Alliances data set

Our methodology is applied to the formal alliances data set (Gibler (2008), v4.1), which records all formal alliances (e.g., mutual defense pacts, non-aggression treaties, and ententes) among different nations between 1816 and 2012. An undirected edge between the two nations indicates that they formed a formal alliance in that year. Studying the global military alliance networks can provide insight into the evolution of geopolitics and international relations across nations over the past two centuries. Visualizing the dynamic networks without a proper statistical model is challenging due to a large number of subjects ($n = 180$ nations) and time points ($T = 197$ years). For example, Park and Sohn (2020) analyzed the data set with only selected years and subjects, both less than 10. Our analysis aims to identify the significant events and countries in history that impacted the global alliance structure and provide a visual summary of these changes over time. While many territories changed during the period, we kept all the nations from the beginning to the end as long as they had at least one alliance at any given time. Therefore, the data set contains all subjects and all time points. The following is an analysis of some of the key

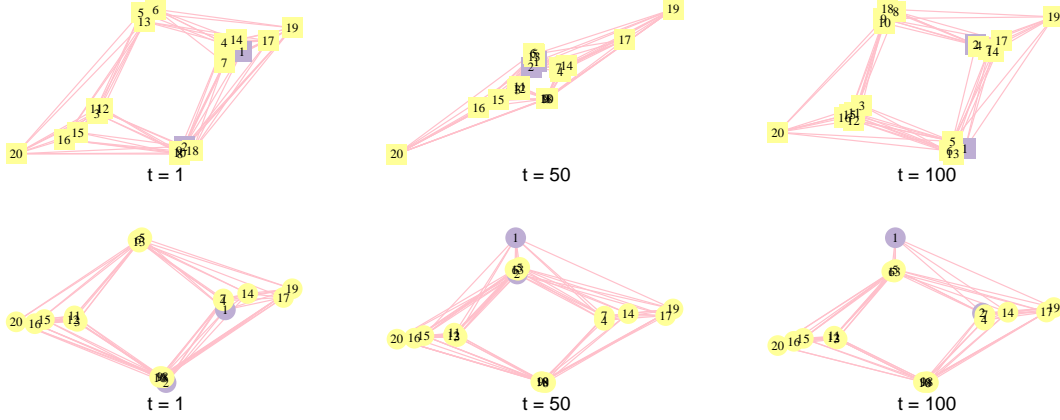


Figure 4: *Snapshots of the estimated latent space for time point 1, 50, 100 where only nodes 1, 2 transit and the rest of the nodes stay static over time. Top row: IGLSM; bottom row: FSS. The estimated latent spaces for FSS are comparable across all time points, which matches the property shown in Corollary 3.3.*

alliances in history. The estimate of the latent vectors is performed via variational means with Procrustes rotation (5).

Figure 6 depicts the formal alliances for 1863 - 1870. Concerning alliances, the most significant historical event was the unification of Germany into the German Empire. The modern German states like Baden, Mecklenburg-Schwerin, Württemberg, Bavaria and Hesse-Darmstadt were independent nations in 1863. As a consequence of the Austro-Prussian War (1866) and the Franco-Prussian War (1870), these states finally merged into Germany (Prussia at the time) due to the development of nationalist sentiments caused by the wars. The figure illustrates the significant changes in the related subjects as a result of the events: In 1865, the estimated locations of the above states formed one cluster with Germany; while starting from 1866, the locations of the above states moved away from Germany after the outbreak of the Austro-Prussian War, as they were on the opposite side to Prussia. Then in 1870, German became adjacent to the above states again since these states fought alongside German against France during the Franco-Prussian War. After merging into German in 1871, the states would not form alliances with other nations the rest of the time. Other major countries like the United Kingdom, France and Austria remained virtually unchanged during the period, reflecting the effect of shrinkage priors.

Figure 7 compares the estimated latent space between 1951 and 1992. From the figure, we can see that the majority of the nodes do not move their positions even though the year gap is large. In addition, the clustering structure also stays similar, reflecting that during the cold war, the NATO and Warsaw Pact almost divided the world and stayed stable. Some significant changes from 1951 to 1992 can also be observed: First, Canada gained

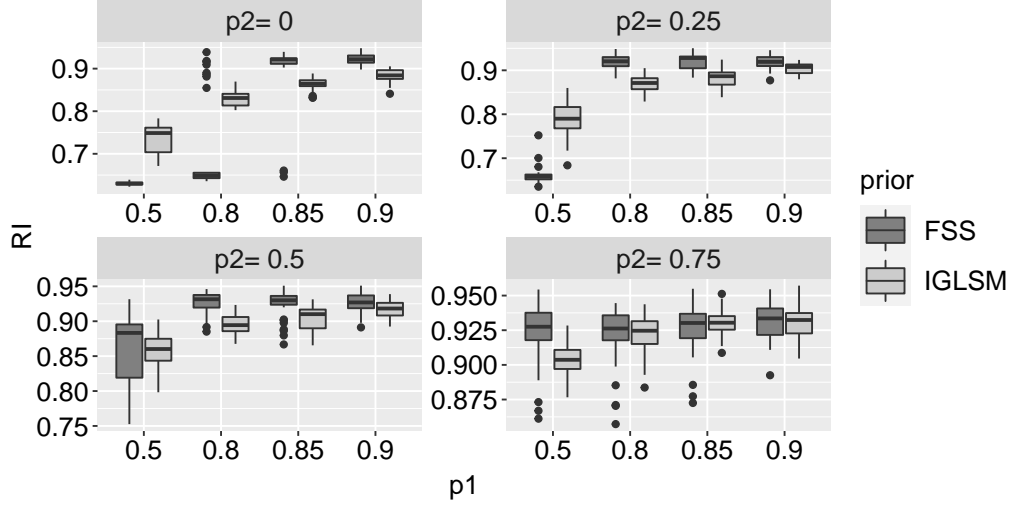


Figure 5: *Boxplot comparing the performance of clustering between FFS and IGLSM. The measure is the median of means of the rand index calculated across 100 time points using K-means over 25 replications. RI: Rand index. FFS performs no worse than IGLSM when the transitions are sparse (except $p_1 = 0.5, 0.8$, $p_2 = 0$ and $p_1 = 0.5, p_2 = 0.25$).*

many connections with South American countries and played a similar role to the US. In addition, Russia’s location also changed significantly, reflecting the end of the cold war on global alliances, where a military alliance between Russia and NATO was established before 1992. As a result of Spain’s membership in NATO in 1982, it moved from its location close to Russia to a cluster of NATO states.

6 Supplementary material

The supplementary material contains two additional real data analysis, the proofs of the main theorems, algorithm details for SMF variational inference and reproducible examples for simulation and real data analysis.

References

- Acharyya, S., Zhang, Z., Bhattacharya, A., and Pati, D. (2018). Bayesian hierarchical modeling on covariance valued data. *arXiv preprint arXiv:1811.00724*.
- Arias-Castro, E., Javanmard, A., and Pelletier, B. (2020). Perturbation bounds for procrustes, classical scaling, and trilateration, with applications to manifold learning. *Journal of machine learning research*, 21:15–1.

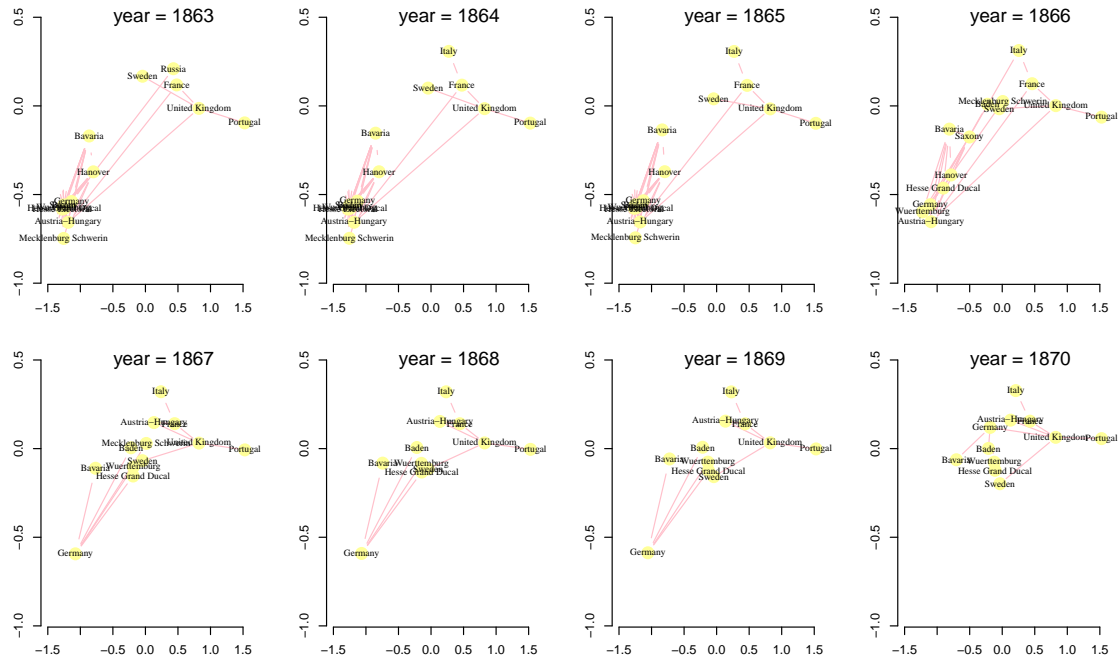


Figure 6: Latent space of world's formal alliances for 1865 - 1872. The locations of names of countries represent the estimated locations of the corresponding subjects after performing Procrustes rotation (5). Some selected labels are shown.

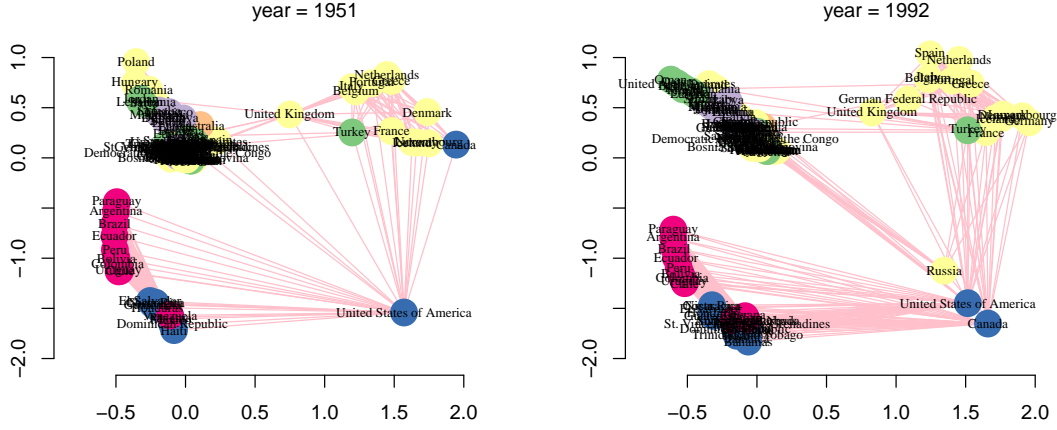


Figure 7: Latent space of world's formal alliances for 1951 and 1992. The locations of names of countries represent the estimated locations of the corresponding subjects after performing Procrustes rotation (5). Some selected labels are shown. Isolated subjects are not shown. Yellow, European countries; red, South American countries; blue, North American countries; Green, Asian countries; Green, African countries; Orange, Australian countries.

- Aßmann, C., Boysen-Hogrefe, J., and Pape, M. (2016). Bayesian analysis of static and dynamic factor models: An ex-post approach towards the rotation problem. *Journal of Econometrics*, 192(1):190–206.
- Bai, Z.-D. and Yin, Y.-Q. (2008). Limit of the smallest eigenvalue of a large dimensional sample covariance matrix. In *Advances In Statistics*, pages 108–127. World Scientific.
- Bashir, A., Carvalho, C. M., Hahn, P. R., and Jones, M. B. (2019). Post-processing posteriors over precision matrices to produce sparse graph estimates. *Bayesian Analysis*, 14(4):1075–1090.
- Bhattacharya, A., Pati, D., and Yang, Y. (2019). Bayesian fractional posteriors. *The Annals of Statistics*, 47(1):39–66.
- Bishop, C. M. and Nasrabadi, N. M. (2006). *Pattern recognition and machine learning*, volume 4. Springer.
- Blei, D. M., Kucukelbir, A., and McAuliffe, J. D. (2017). Variational inference: A review for statisticians. *Journal of the American statistical Association*, 112(518):859–877.
- Buckner, R. L., Krienen, F. M., Castellanos, A., Diaz, J. C., and Yeo, B. T. (2011). The organization of the human cerebellum estimated by intrinsic functional connectivity. *Journal of neurophysiology*, 106(5):2322–2345.

- Carvalho, C. M., Polson, N. G., and Scott, J. G. (2009). Handling sparsity via the horseshoe. In *Artificial Intelligence and Statistics*, pages 73–80. PMLR.
- Chakraborty, A., Bhattacharya, A., and Mallick, B. K. (2020). Bayesian sparse multiple regression for simultaneous rank reduction and variable selection. *Biometrika*, 107(1):205–221.
- Chan, J. C., Koop, G., Leon-Gonzalez, R., and Strachan, R. W. (2012). Time varying dimension models. *Journal of Business & Economic Statistics*, 30(3):358–367.
- Chatterjee, S. (2015). Matrix estimation by universal singular value thresholding. *The Annals of Statistics*, 43(1):177–214.
- Chen, X., He, Z., and Sun, L. (2019). A Bayesian tensor decomposition approach for spatio-temporal traffic data imputation. *Transportation research part C: emerging technologies*, 98:73–84.
- Donoho, D. L., Gavish, M., and Romanov, E. (2020). Screenot: Exact mse-optimal singular value thresholding in correlated noise. *arXiv preprint arXiv:2009.12297*.
- Doukopoulos, X. G. and Moustakides, G. V. (2008). Fast and stable subspace tracking. *IEEE Transactions on Signal Processing*, 56(4):1452–1465.
- Fan, Z. and Guan, L. (2018). Approximate ℓ_0 -penalized estimation of piecewise-constant signals on graphs. *Annals of Statistics*, 46(6B):3217–3245.
- Friel, N., Rastelli, R., Wyse, J., and Raftery, A. E. (2016). Interlocking directorates in irish companies using a latent space model for bipartite networks. *Proceedings of the National Academy of Sciences*, 113(24):6629–6634.
- Frühwirth-Schnatter, S. and Wagner, H. (2010). Stochastic model specification search for gaussian and partial non-gaussian state space models. *Journal of Econometrics*, 154(1):85–100.
- Gavish, M. and Donoho, D. L. (2014). The optimal hard threshold for singular values is $4/\sqrt{3}$. *IEEE Transactions on Information Theory*, 60(8):5040–5053.
- Gibler, D. M. (2008). *International military alliances, 1648-2008*. CQ Press.
- Gil, M., Alajaji, F., and Linder, T. (2013). Rényi divergence measures for commonly used univariate continuous distributions. *Information Sciences*, 249:124–131.
- Gonzalo, J. and Granger, C. (1995). Estimation of common long-memory components in cointegrated systems. *Journal of Business & Economic Statistics*, 13(1):27–35.

- Groen, J. J., Paap, R., and Ravazzolo, F. (2013). Real-time inflation forecasting in a changing world. *Journal of Business & Economic Statistics*, 31(1):29–44.
- Hahn, P. R. and Carvalho, C. M. (2015). Decoupling shrinkage and selection in Bayesian linear models: a posterior summary perspective. *Journal of the American Statistical Association*, 110(509):435–448.
- Harbutt, F. J. (1988). *The iron curtain: Churchill, America, and the origins of the Cold War*. Oxford University Press.
- Hegde, S. R., Manimaran, P., and Mande, S. C. (2008). Dynamic changes in protein functional linkage networks revealed by integration with gene expression data. *PLoS computational biology*, 4(11):e1000237.
- Hitchcock, F. L. (1927). The expression of a tensor or a polyadic as a sum of products. *Journal of Mathematics and Physics*, 6(1-4):164–189.
- Hochreiter, S. and Schmidhuber, J. (1997). Long short-term memory. *Neural computation*, 9(8):1735–1780.
- Hoff, P. D. (2007). Model averaging and dimension selection for the singular value decomposition. *Journal of the American Statistical Association*, 102(478):674–685.
- Hoff, P. D. (2011). Hierarchical multilinear models for multiway data. *Computational Statistics & Data Analysis*, 55(1):530–543.
- Hoff, P. D. (2015). Multilinear tensor regression for longitudinal relational data. *The Annals of applied statistics*, 9(3):1169.
- Huang, X., Wang, J., and Liang, F. (2016). A variational algorithm for Bayesian variable selection. *arXiv preprint arXiv:1602.07640*.
- Jaakkola, T. S. and Jordan, M. I. (2000). Bayesian parameter estimation via variational methods. *Statistics and Computing*, 10(1):25–37.
- Kalli, M. and Griffin, J. E. (2014). Time-varying sparsity in dynamic regression models. *Journal of Econometrics*, 178(2):779–793.
- Kalman, R. E. (1960). A New Approach to Linear Filtering and Prediction Problems. *Journal of Basic Engineering*, 82(1):35–45.
- Kowal, D. R., Matteson, D. S., and Ruppert, D. (2019). Dynamic shrinkage processes. *Journal of the Royal Statistical Society: Series B (Statistical Methodology)*, 81(4):781–804.

- Lee, D. S., Moretti, E., and Butler, M. J. (2004). Do voters affect or elect policies? evidence from the us house. *The Quarterly Journal of Economics*, 119(3):807–859.
- Lee, K. and Lee, J. (2021). Post-processed posteriors for sparse covariances and its application to global minimum variance portfolio. *arXiv preprint arXiv:2108.09462*.
- Lei, J. and Rinaldo, A. (2015). Consistency of spectral clustering in stochastic block models. *The Annals of Statistics*, 43(1):215–237.
- Liu, F., Choi, D., Xie, L., and Roeder, K. (2018). Global spectral clustering in dynamic networks. *Proceedings of the National Academy of Sciences*, 115(5):927–932.
- Lütkepohl, H. (2013). Vector autoregressive models. In *Handbook of Research Methods and Applications in Empirical Macroeconomics*, pages 139–164. Edward Elgar Publishing.
- Massart, P. (2007). *Concentration inequalities and model selection*, volume 6. Springer.
- Nakajima, J. and West, M. (2013). Bayesian analysis of latent threshold dynamic models. *Journal of Business & Economic Statistics*, 31(2):151–164.
- Nasiri, M., Rezghi, M., and Minaei, B. (2014). Fuzzy dynamic tensor decomposition algorithm for recommender system. *UCT Journal of Research in Science, Engineering and Technology*, 2(2):52–55.
- Neville, S. E., Ormerod, J. T., and Wand, M. (2014). Mean field variational Bayes for continuous sparse signal shrinkage: pitfalls and remedies. *Electronic Journal of Statistics*, 8(1):1113–1151.
- Ng, A., Jordan, M., and Weiss, Y. (2001). On spectral clustering: Analysis and an algorithm. *Advances in neural information processing systems*, 14.
- Palma, W. (2007). *Long-memory time series: theory and methods*. John Wiley & Sons.
- Papastamoulis, P. and Ntzoufras, I. (2022). On the identifiability of Bayesian factor analytic models. *Statistics and Computing*, 32(2):1–29.
- Park, J. H. and Sohn, Y. (2020). Detecting structural changes in longitudinal network data. *Bayesian Analysis*, 15(1):133–157.
- Pensky, M. and Zhang, T. (2019). Spectral clustering in the dynamic stochastic block model. *Electronic Journal of Statistics*, 13(1):678–709.
- Ray, K. and Szabó, B. (2021). Variational Bayes for high-dimensional linear regression with sparse priors. *Journal of the American Statistical Association*, pages 1–12.
- Robinson, P. M. (2003). *Time series with long memory*. Advanced Texts in Econometrics.

- Sarkar, P. and Moore, A. W. (2005). Dynamic social network analysis using latent space models. *Acm Sigkdd Explorations Newsletter*, 7(2):31–40.
- Sewell, D. K. and Chen, Y. (2015). Latent space models for dynamic networks. *Journal of the American Statistical Association*, 110(512):1646–1657.
- Sewell, D. K. and Chen, Y. (2017). Latent space approaches to community detection in dynamic networks. *Bayesian analysis*, 12(2):351–377.
- Sun, J. Z., Parthasarathy, D., and Varshney, K. R. (2014). Collaborative kalman filtering for dynamic matrix factorization. *IEEE Transactions on Signal Processing*, 62(14):3499–3509.
- Sun, J. Z., Varshney, K. R., and Subbian, K. (2012). Dynamic matrix factorization: A state space approach. In *2012 IEEE International Conference on Acoustics, Speech and Signal Processing (ICASSP)*, pages 1897–1900. IEEE.
- Tan, H., Wu, Y., Shen, B., Jin, P. J., and Ran, B. (2016). Short-term traffic prediction based on dynamic tensor completion. *IEEE Transactions on Intelligent Transportation Systems*, 17(8):2123–2133.
- Thomas Yeo, B., Krienen, F. M., Sepulcre, J., Sabuncu, M. R., Lashkari, D., Hollinshead, M., Roffman, J. L., Smoller, J. W., Zöllei, L., Polimeni, J. R., et al. (2011). The organization of the human cerebral cortex estimated by intrinsic functional connectivity. *Journal of neurophysiology*, 106(3):1125–1165.
- Tsybakov, A. B. (2008). *Introduction to nonparametric estimation*. Springer Science & Business Media.
- Vershynin, R. (2010). Introduction to the non-asymptotic analysis of random matrices. *arXiv preprint arXiv:1011.3027*.
- Von Luxburg, U. (2007). A tutorial on spectral clustering. *Statistics and computing*, 17(4):395–416.
- Walker, S. and Hjort, N. L. (2001). On Bayesian consistency. *Journal of the Royal Statistical Society: Series B (Statistical Methodology)*, 63(4):811–821.
- Yu, M., Gupta, V., and Kolar, M. (2020). Recovery of simultaneous low rank and two-way sparse coefficient matrices, a nonconvex approach. *Electronic Journal of Statistics*, 14(1):413–457.
- Zhang, R., Lin, C. D., and Ranjan, P. (2018). Local gaussian process model for large-scale dynamic computer experiments. *Journal of Computational and Graphical Statistics*, 27(4):798–807.

- Zhang, Y., Bi, X., Tang, N., and Qu, A. (2021). Dynamic tensor recommender systems. *Journal of Machine Learning Research*, 22(65):1–35.
- Zhou, H., Li, L., and Zhu, H. (2013). Tensor regression with applications in neuroimaging data analysis. *Journal of the American Statistical Association*, 108(502):540–552.
- Zhu, L., Guo, D., Yin, J., Ver Steeg, G., and Galstyan, A. (2016). Scalable temporal latent space inference for link prediction in dynamic social networks. *IEEE Transactions on Knowledge and Data Engineering*, 28(10):2765–2777.

7 Appendix

7.1 Additional simulations real data analysis

7.1.1 Additional simulations

Case 2, Binary network model: $n = 5, 10, 20, 50$:

$$\begin{aligned} \mathbf{u}_{i1} &\sim 0.5\mathcal{N}((1, 0)', \mathbb{I}) + 0.5\mathcal{N}((-1, 0)', \mathbb{I}), \quad i = 1, \dots, n \\ D\mathbf{u}_{it} &= \begin{cases} (0, 0)' & \text{with probability } \rho \\ (-0.25, -0.25)' & \text{with probability } (1 - \rho)/2 \\ (0.25, 0.25)' & \text{with probability } (1 - \rho)/2. \end{cases} \quad i = 1, \dots, n; t = 2, \dots, T \\ Y_{ijt} &\sim \text{Ber}(\text{logistic}(-\mathbf{u}_{it}'\mathbf{u}_{jt})) \quad i > j; \quad Y_{ijt} = Y_{jit}, t = 1, \dots, T. \end{aligned}$$

Case 3, Gaussian Tensor model: $M = 3, n_1, n_2, n_3 = 5, 10, n_1 \geq n_2 \geq n_3$:

$$\begin{aligned} \mathbf{u}_{i1}^{(m)} &\sim \mathcal{N}(\mathbf{0}, \mathbb{I}), \quad i = 1, \dots, n_m, m = 1, 2, 3 \\ D\mathbf{u}_{it}^{(m)} &= \begin{cases} (0, 0)' & \text{with probability } \rho \\ (-0.25, -0.25)' & \text{with probability } (1 - \rho)/2 \\ (0.25, 0.25)' & \text{with probability } (1 - \rho)/2, \end{cases} \quad m = 1, 2, 3 \\ &\quad i = 1, \dots, n_m; t = 2, \dots, T \\ \mathcal{Y}_t &\sim \mathcal{N}\left(\sum_{l=1}^d \mathbf{u}_{t,l}^{(1)} \otimes \mathbf{u}_{t,l}^{(2)} \otimes \mathbf{u}_{t,l}^{(3)}, 0.3^2\right) \quad i = 1, \dots, n_m, m = 1, 2, 3; t = 1, \dots, T. \end{aligned}$$

According to the simulation results from Table 1, when $\rho \geq 0.85$ increases, FFS, SVD and SVD2 improve estimation accuracy. The phenomenon occurs because the Bernoulli distribution has a smaller variance if the probabilities are close to zero or one. In addition, the initial distribution is generated from a mixture distribution with separate components that generate true probabilities close to zero or one. Consequently, if ρ becomes larger, then the true binary responses for $t = 2, \dots, T$ also tend to have probabilities close to 0 or 1, making it easier to obtain higher accuracy for the entire problem. Nevertheless, the proposed method still outperforms SVD and SVD2 in terms of PCC in almost all cases for $\rho \geq 0.8$. The results indicate that the proposed approach can benefit from the time dependence induced by fusion structure as ρ increases, which cannot be ascribed to SVD and SVD2. When the sparsity assumption is violated with $\rho = 0.5$, the proposed method is still comparable to SVD and SVD2. Next, Table 2 compares FFS with CP decomposition for tensor data generated in Case 3. FFS performs better than CP across all simulation settings. Note that CP decomposition is optimized through alternating least squares, which is in a similar fashion to the CAVI algorithm. Therefore, both methods suffer from some bad local optimal induced by the alternating optimization mechanism. Therefore, the improvement in the estimation of FFS is simply because the fusion structure is taken into account.

Table 1: Performance comparison for binary cases between FFS and SVD. The measure is the median PCC for estimation of the connected probabilities.

| n | Method | ρ | | | | | |
|-----|--------|--------------|--------------|--------------|--------------|--------------|--------------|
| | | 0.5 | 0.8 | 0.85 | 0.9 | 0.95 | 0.99 |
| 5 | FFS | 0.909 | 0.867 | 0.920 | 0.959 | 0.984 | 0.990 |
| | SVD | 0.774 | 0.758 | 0.771 | 0.735 | 0.726 | 0.737 |
| | SVD2 | 0.531 | 0.579 | 0.755 | 0.709 | 0.476 | 0.690 |
| 10 | FFS | 0.956 | 0.959 | 0.951 | 0.940 | 0.949 | 0.953 |
| | SVD | 0.864 | 0.833 | 0.833 | 0.829 | 0.876 | 0.889 |
| | SVD2 | 0.829 | 0.819 | 0.844 | 0.852 | 0.884 | 0.881 |
| 20 | FFS | 0.973 | 0.980 | 0.985 | 0.985 | 0.994 | 0.999 |
| | SVD | 0.919 | 0.941 | 0.947 | 0.959 | 0.957 | 0.950 |
| | SVD2 | 0.938 | 0.949 | 0.957 | 0.967 | 0.965 | 0.963 |
| 50 | FFS | 0.970 | 0.985 | 0.984 | 0.992 | 0.996 | 0.997 |
| | SVD | 0.934 | 0.967 | 0.936 | 0.970 | 0.973 | 0.973 |
| | SVD2 | 0.972 | 0.975 | 0.960 | 0.978 | 0.979 | 0.981 |

Table 2: Performance comparison for tensor cases between FFS and CP decomposition. The measure is the median RMSE for estimation of the \mathcal{M} .

| (n_1, n_2, n_3) | Method | ρ | | | | | |
|-------------------|--------|--------------|--------------|--------------|--------------|--------------|--------------|
| | | 0.5 | 0.8 | 0.85 | 0.9 | 0.95 | 0.99 |
| (5 ,5 ,5) | FFS | 0.132 | 0.119 | 0.119 | 0.121 | 0.127 | 0.113 |
| | CP | 0.187 | 0.147 | 0.153 | 0.145 | 0.148 | 0.143 |
| (10 ,5 ,5) | FFS | 0.114 | 0.107 | 0.102 | 0.106 | 0.103 | 0.104 |
| | CP | 0.213 | 0.127 | 0.132 | 0.117 | 0.117 | 0.121 |
| (10 ,10 ,5) | FFS | 0.093 | 0.088 | 0.087 | 0.082 | 0.081 | 0.074 |
| | CP | 0.159 | 0.121 | 0.111 | 0.092 | 0.092 | 0.092 |
| (10 ,10 ,10) | FFS | 0.073 | 0.068 | 0.069 | 0.067 | 0.067 | 0.065 |
| | CP | 0.192 | 0.072 | 0.073 | 0.071 | 0.071 | 0.072 |

7.2 Formal alliances data

Figure 9 shows an early formulation of the North Atlantic Treaty Organization (NATO). The United States formed an alliance with a list of American countries in 1948, known as the Inter-American Treaty of Reciprocal Assistance. It can be seen from the graph that the United States belongs to the cluster around many south American countries in 1948. With the formation of NATO in 1949, the United States drastically changed its location and gained connectivity with NATO’s European members. The connectivity status of the United States demonstrated its strong influence in both America and Europe. From

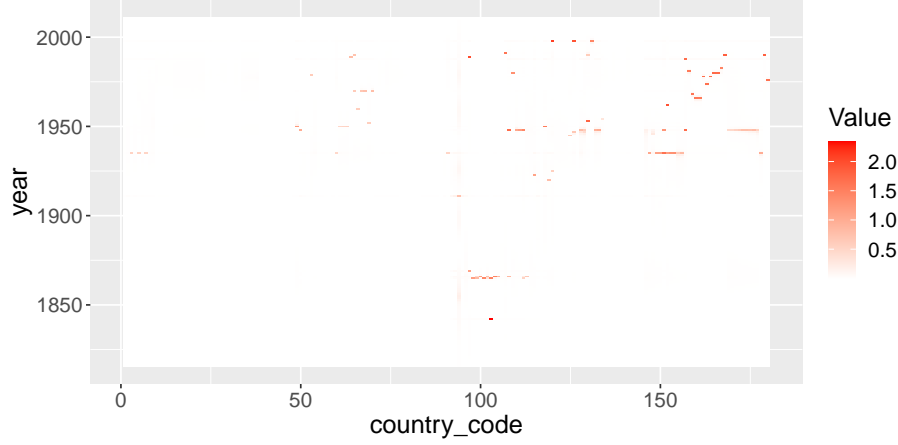


Figure 8: Heatmaps of matrices whose components are ℓ_2 norm of transitions $\{\|D\mathbf{u}_{it}\|\}_{i,t}$ after estimating latent vectors by FFS priors. *country_code*: 1-48: Africa countries; 49-89 Asian countries; 90-91: Australian countries; 92-145: European countries; 146-168: North American countries; 169-180: South American countries. *year*: year of the transitions.

1950 to 1951, significant changes also occurred for Turkey, which dropped from close to Russia to close to France. The move indicated the participation of Turkey in NATO during 1951-1952. Figure 10 depicts the end of the Cold War. Note that most of the locations in 1989 remained almost unchanged from those in 1949 in Figure 9, revealing a relatively stable network structure after 1949. A significant shift in Russia’s location occurred in 1992, reflecting the end of the cold war on global alliances. Specifically, the Treaty on Conventional Armed Forces in Europe entered into force in 1992, and established a military alliance between Russia and NATO. During the period from 1990 to 1992, the movement of German Federal Republic also reflected the German reunification.

7.2.1 HCP motor task data

The HCP motor task experiment was designed by Buckner et al. (2011) and Thomas Yeo et al. (2011). In the experiment, a series of visual cues are presented to participants requesting them to tap their left or right fingers, squeeze their left or right toes, or move their tongues to map motor areas. The experiment consists of 13 blocks, with 4 hand movements (2 right and two left), 4 foot movements (2 right and two left), and 2 tongue movements, together with 3 fixation blocks between tasks. A time series of 10×10 covariance matrices with 26 time points were generated from ten cortical ROIs (region of interests) related to motor control around the motor strip area, including left and right postcentral gyri, pre-central gyri, and central gyrus. The investigation contains 500 subjects of such dynamic matrices.

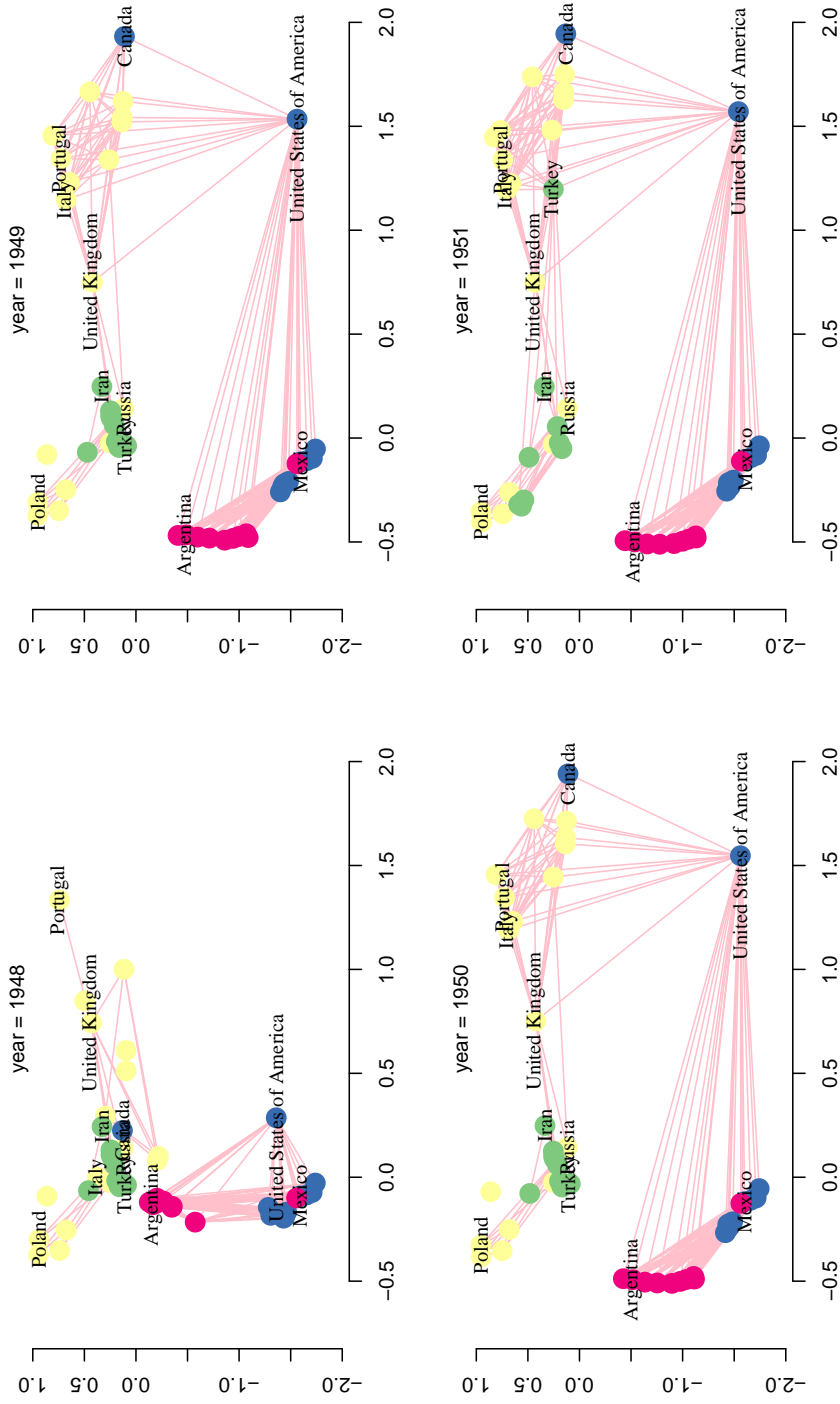


Figure 9: Latent space of world's formal alliances for 1948 - 1951. The locations of names of countries represent the estimated locations of the corresponding subjects after performing Procrustes rotation (5). Some selected labels are shown. Isolated subjects are not shown. Yellow, European countries; red, South American countries; blue, North American countries; Green, Asian countries; Orange, African countries; Pink, Australian countries.

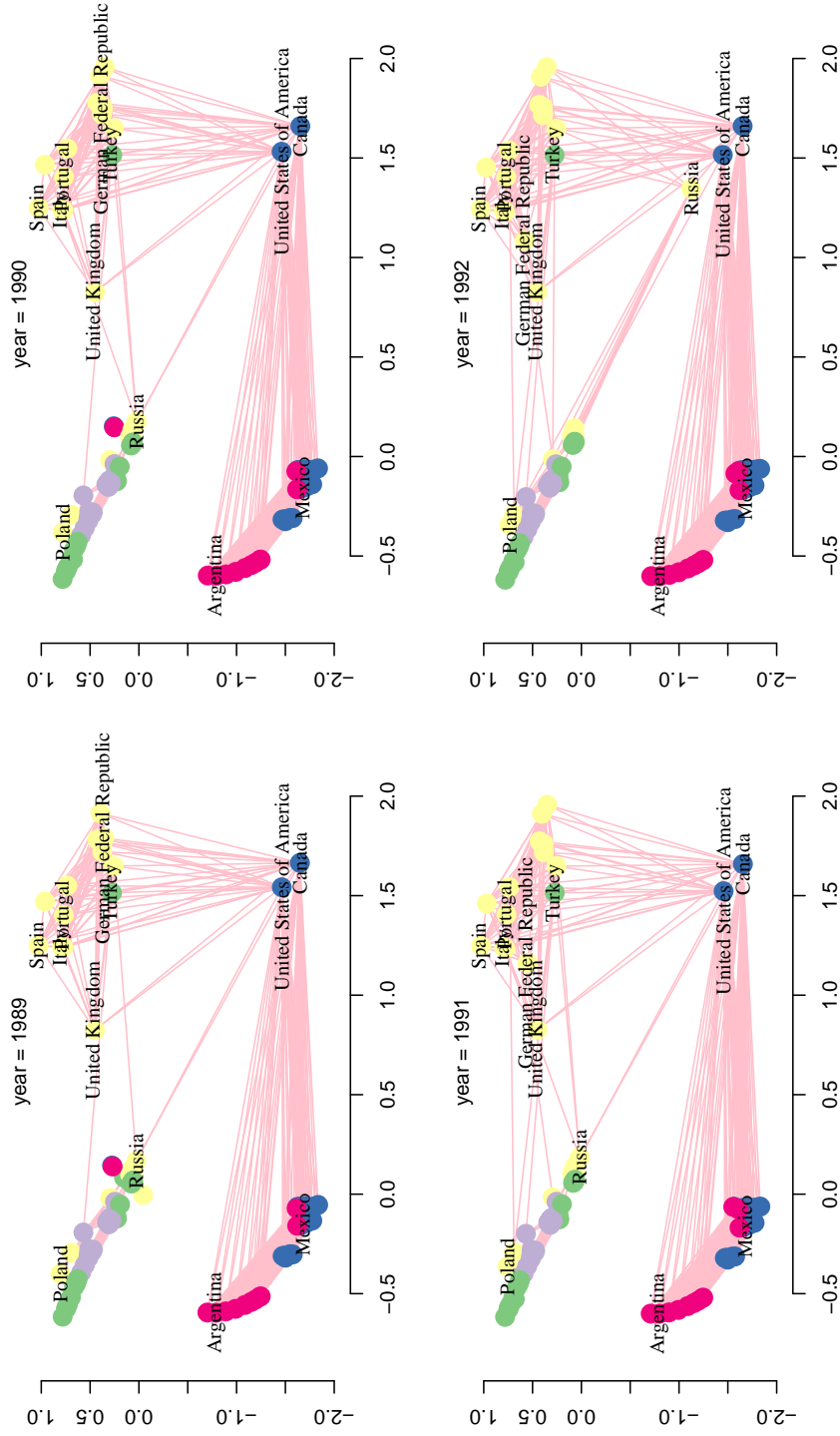


Figure 10: Latent space of world's formal alliances for 1989 - 1992. The locations of names of countries represent the estimated locations of the corresponding subjects after performing Procrustes rotation (5). Some selected labels are shown. Isolated subjects are not shown. Yellow, European countries; red, South American countries; blue, North American countries; Green, Asian countries; Orange, African countries; Purple, Australian countries.

We first convert all the covariance matrices to correlation matrices, and directly consider the correlation matrix as a Gaussian network, where $Y_{ijt} \sim \mathcal{N}(\mathbf{u}'_{it}\mathbf{u}_{jt}, \sigma^2)$ for $i > j, t = 1, \dots, 26$. We apply FFS with $d = 2$, and the variance σ is learned by putting additional inverse-gamma prior $\text{IG}(1/2, 1/2)$. To detect important transitions of the covariance matrices, we record the time when the overall transitions of all subjects are the largest (in ℓ_2 norm) in the variational estimations for all 500 subjects, as long as the transitions of all subjects are not too small (at least one should $\geq 1e - 4$). Figure 11 shows the histogram of the detected important time points. It can be seen that the change point concentrates on time around 4, 14, 23. Note that the change point 23 is also detected in other literature (Acharyya et al., 2018) using the same data via a different modeling approach. In addition, 4 is the mirror point of 23 considering the task, asserting that a similar scenario happens at the beginning of the experiment. Finally, 14 is close to the mid-point of the overall period. This validated the fact that the experiment consisted of three different tasks, and the detected change points can be explained by the change points of three different tasks.

7.3 Simulation settings for Figure 1

Let $d = 2, n = 10, T = 100$. The initial distribution of each component of the true latent vectors is uniformly sampled from $\{(-1, -1)', (-1, 1)', (1, -1)', (1, 1)'\}$. The subjects 1 and 2 transit with probability 0.05 at each time point, while the rest of subjects stay static across all time. Data is then generated according to the model: $Y_{ijt} \sim \text{Ber}(\text{logistic}(-2\mathbf{u}'_{it}\mathbf{u}_{jt})), i > j; Y_{ijt} = Y_{jit}, t = 1, \dots, T$.

7.4 Comparison of the MP algorithm to proximal gradient for ℓ_1 penalized trend filtering

Due to the fact that the variational family (10) captures the temporal dependence, the computation of $q(\boldsymbol{\theta})$ given the rest densities can be carried out in a message-passing manner. The proposed VI algorithm converges faster than the proximal gradient descent algorithm for ℓ_1 regularized trend filtering problem without increasing the complexity of computation and storage per iteration due to the fact that message-passing utilizes the banded (block tri-diagonal) structure of the second-order moments, which can be inverted at an $O(Td^3)$ cost. Figure 12 provides a simulation example by comparing our convergence in iterations between the proposed VI approach and the proximal and accelerated proximal gradient descent for a trend-filtering problem with ℓ_1 regularization for $d = 1$.

7.5 Proof of Theorem 3.1

Proof. For $\Theta^a = [\mathcal{U}^{a'}, \mathcal{V}^{a'}]'$ and $\Theta^b = [\mathcal{U}^{b'}, \mathcal{V}^{b'}]'$, let

$$d^2(\Theta^a, \Theta^b) = \sum_{t=1}^T \|\mathbf{U}_t^a \mathbf{V}_t^{a'} - \mathbf{U}_t^b \mathbf{V}_t^{b'}\|_F^2,$$

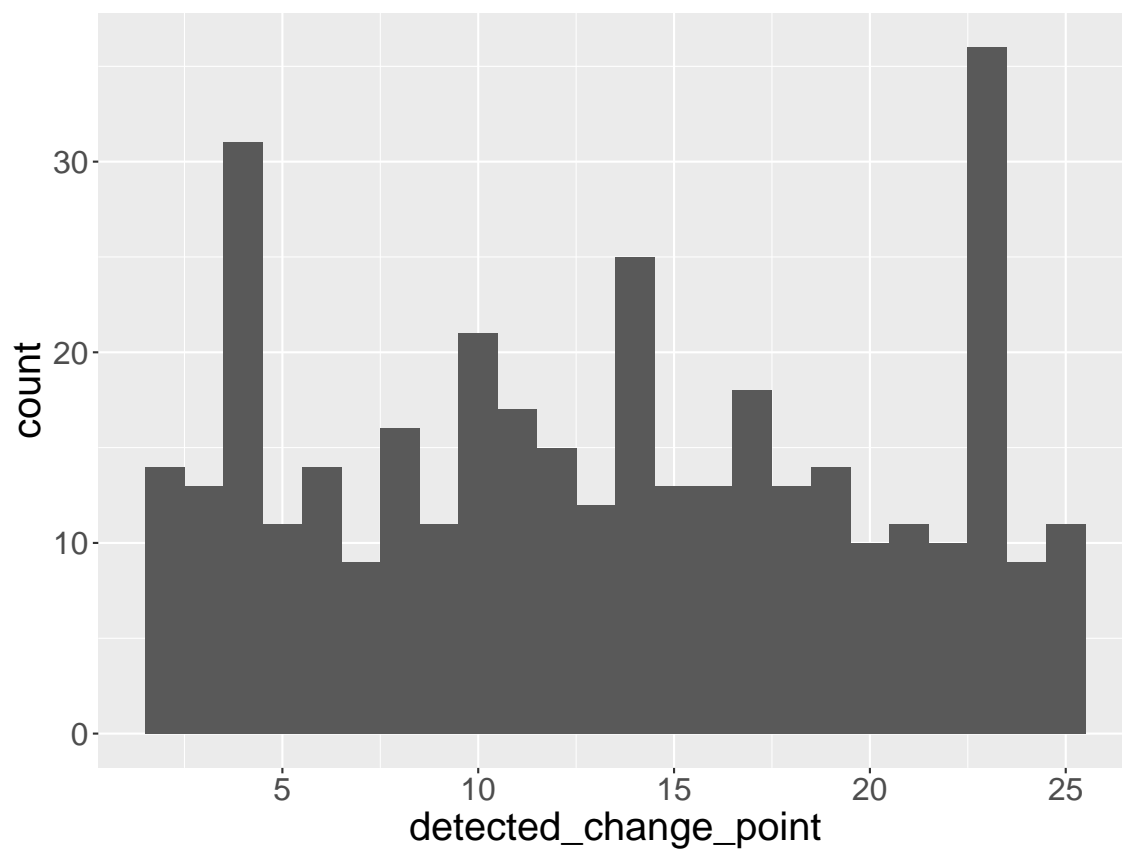


Figure 11: Detected time points for large transitions across all 500 subjects.

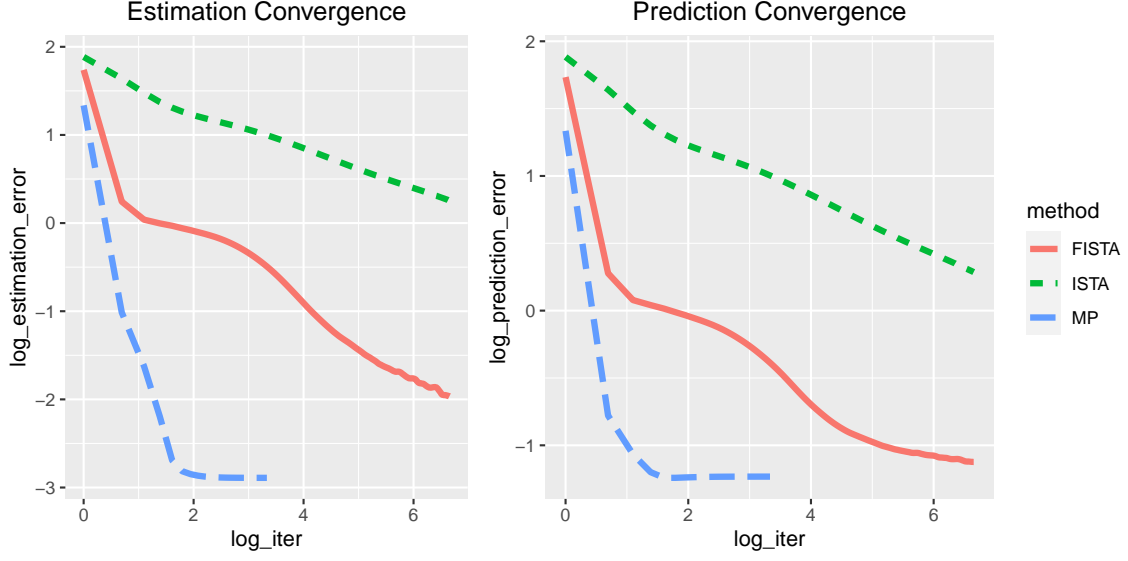


Figure 12: Comparison in iterations between message passing variational inference under proposed prior vs. proximal (ISTA) and accelerated proximal gradient descent (FISTA) under ℓ_1 regularized trend filter problem. The hyperparameter τ of FFS are assigned with a fixed value to avoid model selection for fair comparison.

and

$$d_0^2(\mathbf{U}_t^a \mathbf{V}_t^{a'}, \mathbf{U}_t^b \mathbf{V}_t^{b'}) = \|\mathbf{U}_t^a \mathbf{V}_t^{a'} - \mathbf{U}_t^b \mathbf{V}_t^{b'}\|_F^2.$$

The hypothesis set is constructed such that all elements are sufficiently distinct and the cardinality of the set can be constrained.

7.5.1 Asymmetric case:

To obtain the final bound for the asymmetric case, we use an alternative strategy. Initially, we fix \mathcal{V} and select a suitable parameter space for \mathcal{U} to obtain a rate of the lower bound; we then fix \mathcal{U} and construct a hypothesis space for \mathcal{V} to obtain a second lower bound. The final rate of the lower bound should be the sum of the two.

As a first step, we should first obtain a sparse Varshamov-Gilbert bound in Lemma 7.1 under Hamming distance for the low-rank subset construction:

Lemma 7.1 (Lemma 4.10 in Massart (2007)). *Let $\Omega = \{0, 1\}^n$ and $1 \leq n_0 \leq n/4$. Then there exists a subset $\{\mathbf{w}^{(1)}, \dots, \mathbf{w}^{(M)}\} \subset \Omega$ such that*

1. $\|\mathbf{w}^{(i)}\|_0 = n_0$ for all $1 \leq i \leq M$;
2. $\|\mathbf{w}^{(i)} - \mathbf{w}^{(j)}\|_0 \geq n_0/2$ for $0 \leq i \neq j \leq M$;

3. $\log M \geq cn_0 \log(n/n_0)$ with $c \geq 0.233$.

We construct the following case according to Lemma 7.1 (the construction holds under $n - d + 1 \geq 4$). For each \mathbf{w} , we can construct an $n \times d$ matrix and a $p \times d$ matrix as follows:

$$\mathbf{U}^w = \begin{bmatrix} \epsilon \mathbf{w} & \mathbf{0} \\ \mathbf{0} & \mathbf{I}_{d-1} \end{bmatrix} \quad \text{with } w \in \Omega_M; \quad \mathbf{V}^0 = \begin{bmatrix} \mathbf{1}_{p-d+1} & \mathbf{0} \\ \mathbf{0} & \mathbf{I}_{d-1} \end{bmatrix},$$

which gives

$$\mathbf{U}^w \mathbf{V}^{0'} = \begin{bmatrix} \epsilon \mathbf{w} \mathbf{1}' & \mathbf{0} \\ \mathbf{0} & \mathbf{I}_{d-1} \end{bmatrix}.$$

The effect of this construction is that: for different $\mathbf{w}_1, \mathbf{w}_2 \in \Omega_M$, since $n_0/2 \leq \|\mathbf{w}_1 - \mathbf{w}_2\|_0 \leq 2n_0$ and $\|\mathbf{V}^0\|_F \leq \sqrt{p}$, we have

$$d_0(\mathbf{U}^{w_1} \mathbf{V}^{0'}, \mathbf{U}^{w_2} \mathbf{V}^{0'}) \leq \|\mathbf{U}^{w_1} - \mathbf{U}^{w_2}\|_F \|\mathbf{V}^0\|_F = \sqrt{n} \epsilon \|\mathbf{w}_1 - \mathbf{w}_2\|_2 \leq \sqrt{2pn_0} \epsilon.$$

In addition, note that

$$d_0^2(\mathbf{U}^{w_1} \mathbf{V}^{0'}, \mathbf{U}^{w_2} \mathbf{V}^{0'}) = (p - d - 1) \epsilon^2 \sum_{i=1}^{n_0} (w_{1i} - w_{2i})^2 \geq \frac{n_0(p - d - 1) \epsilon^2}{2}.$$

Let

$$\mathbf{U}^0 = \begin{bmatrix} \mathbf{0} & \mathbf{0} \\ \mathbf{0} & \mathbf{I}_{d-1} \end{bmatrix}$$

$$\mathcal{U}^0 = [\mathbf{U}^0, \dots, \mathbf{U}^0], \mathcal{V}^0 = [\mathbf{V}^0, \dots, \mathbf{V}^0] \text{ and } \Theta^0 = [\mathcal{U}^{0'}, \mathcal{V}^{0'}]'$$

We need the above Varshamov-Gilbert Bound 7.1 again to introduce another binary coding:

Let $\Omega_r = \{\phi^{(1)}, \dots, \phi^{(M_0)}\} \subset \{0, 1\}^T$, such that $\|\phi^{(i)}\|_0 = t_0$ for all $1 \leq i \leq M_0$ and $\|\phi^{(i)} - \phi^{(j)}\|_0 \geq t_0/2$ for $0 \leq i < j \leq M_0$ with $\log M_0 \geq ct_0 \log(T/t_0)$ with $c \geq 0.233$.

Then we have the following construction:

$$\begin{aligned} \Xi_\epsilon &= \{\Theta^{(w, \phi)} : \\ &\quad \mathbf{U}_t^{(w, \phi)} = \mathbf{U}^{w^{(i)}}, \quad \text{if } \phi_t = 1, \\ &\quad \mathbf{U}_t^{(w, \phi)} = \mathbf{U}^0, \quad \text{if } \phi_t = 0, \\ &\quad \mathbf{V}_t^{(w, \phi)} = \mathbf{V}_0, \\ &\quad \mathbf{w}^{(i)} \in \Omega_M, \forall i = 1, \dots, t_0, \mathbf{w}^{(i)} \text{ is chosen with replacement, } \phi \in \Omega_r\}, \end{aligned}$$

For example, when $\phi = (0, 1, 0, 1, 0, 1, \dots)$, $\mathbf{U}_1^{(w, \phi)}, \dots, \mathbf{U}_T^{(w, \phi)}$ is:

$$\begin{bmatrix} \mathbf{U}^0 \\ \mathbf{V}^0 \end{bmatrix}, \begin{bmatrix} \mathbf{U}^{w^{(1)}} \\ \mathbf{V}^0 \end{bmatrix}, \begin{bmatrix} \mathbf{U}^0 \\ \mathbf{V}^0 \end{bmatrix}, \begin{bmatrix} \mathbf{U}^{w^{(2)}} \\ \mathbf{V}^0 \end{bmatrix}, \begin{bmatrix} \mathbf{U}^0 \\ \mathbf{V}^0 \end{bmatrix}, \begin{bmatrix} \mathbf{U}^{w^{(3)}} \\ \mathbf{V}^0 \end{bmatrix}, \dots$$

For $\Theta^{(w_1, \phi_1)}, \Theta^{(w_2, \phi_2)} \in \Xi_\epsilon$, we have

$$d^2(\Theta^{(w_1, \phi_1)}, \Theta^{(w_2, \phi_2)}) = \sum_{t=1}^T d_0^2(\mathbf{U}_t^{(w_1, \phi_1)} \mathbf{V}^{0'}, \mathbf{U}_t^{(w_2, \phi_2)} \mathbf{V}^{0'}) \geq \frac{t_0 n_0 (p - d + 1)}{4} \epsilon^2.$$

We have

$$|\Xi_\epsilon| = M_0 M^{t_0}, \quad \text{with} \quad \log(|\Xi_\epsilon|) \geq c t_0 n_0 \log((n - d - 1)/n_0) + c_0 t_0 \log(T/t_0).$$

In addition, the KL divergence between any elements $\Theta \in \Xi_\epsilon$ and Θ^0 can be upper bounded:

$$D_{KL}(P_\Theta \| P_{\Theta^0}) \leq C_0 d^2(\Theta, \Theta^0) \leq C_0 t_0 n_0 (p - d - 1) \epsilon^2,$$

for some constant $C_0 > 0$.

Based on the construction, we have for $\Theta \in \Xi_\epsilon$, $\sum_{t=2}^T \mathbb{1}\{D\mathbf{u}_{it} \neq 0\} \leq 2t_0$ for $i = 1, \dots, n$ and $\sum_{i=1}^n \mathbb{1}\{D\mathbf{u}_{it} \neq 0\} \leq 2n_0$ for $t = 2, \dots, T$. Therefore we have

$$\sum_{i=1}^n \sum_{t=2}^T \mathbb{1}\{D\mathbf{u}_{it} \neq 0\} \leq 4t_0 n_0.$$

We use the following Lemma 7.2 to show final prove that the minimax rate holds:

Lemma 7.2 (Theorem 2.5 in [Tsybakov \(2008\)](#)). *Suppose $M \geq 2$ and (Θ, d) contains elements $\theta_0, \dots, \theta_M$ such that $d(\theta_i, \theta_j) \geq 2s > 0$ for any $0 \leq i \leq j \leq M$ and $\sum_{i=1}^M D_{KL}(P_{\theta_i}, P_0)/M \leq \alpha \log M$ with $0 < \alpha < 1/8$. Then we have*

$$\inf_{\hat{\theta}} \sup_{\theta \in \Theta} P_{\hat{\theta}}(d(\hat{\theta}, \theta) \geq s) \geq \frac{\sqrt{M}}{1 + \sqrt{M}} \left(1 - 2\alpha - \sqrt{\frac{2\alpha}{\log M}} \right).$$

We consider different cases such that by choosing different t_0, n_0 , the constraint $4t_0 n_0 \leq s_u$ and the KL is upper bounded by the log cardinality (up to constant factor) can both be satisfied:

$$\begin{cases} 4t_0 n_0 & \leq s_u; \\ t_0 n_0 (p - d - 1) \epsilon^2 & \lesssim t_0 n_0 \log((n - d - 1)/n_0) + t_0 \log(T/t_0). \end{cases} \quad (11)$$

Sparse rate ($s_u \leq T$):

When $s_u \leq T$. Denote $n_0 = 1$ and $t_0 = s_u/4$, which satisfies $4n_0 t_0 \leq s_u$. Then it's enough to set

$$s_u (p - d - 1) \epsilon^2 \lesssim s_u \log(4T/s_u) + s_u \log(n - d - 1).$$

Sparse rate ($s_u > T$):

First, suppose $(n-d-1)T/4 > s_u > T$, we assume s_u/T is an integer for simplicity. Let $n_0 = s_u/T$ and $t_0 = T/4$, which satisfies $4n_0t_0 \leq s_u$. To adopt the above Lemma 7.2, it suffices to show

$$n_0t_0(p-d-1)\epsilon^2 \leq \alpha \log(M_0M^{T/4}) = \alpha \log(|\Xi_\epsilon|),$$

with $\alpha < 1/8$. Then we only need to set

$$s_u(p-d-1)\epsilon^2 \lesssim T \log 4 + s_u \log \left(\frac{(n-d-1)T}{s_u} \right).$$

By taking $\epsilon = c^* \sqrt{\log(nT/s_u)/(p-d-1)}$ for some constant $c^* > 0$ such that the above inequality is satisfied, we have

$$\frac{t_0n_0(p-d+1)\epsilon^2}{4} \gtrsim s_u \log(Tn/s_u).$$

By taking $\epsilon = c^* \sqrt{\log(Tn/s_u)/(p-d-1)}$ for some constant $c^* > 0$, we have

$$\frac{t_0n_0(p-d+1)\epsilon^2}{4} \gtrsim s_u \log(Tn/s_u).$$

Dense rate:

If $s_u \geq (n-d-1)T/4$, the difference between latent vectors is dense instead. Then we assign $n_0 = (n-d-1)/2$ and $t_0 = T/2$, which satisfies the constraint. In this case, we need to set

$$(p-d-1)Tn\epsilon^2 \lesssim T + T(n-d-1).$$

By taking $\epsilon = c^* \sqrt{1/(p-d-1)}$ for some constant $c^* > 0$ such that the above inequality is satisfied, we have

$$\frac{t_0n_0(p-d+1)\epsilon^2}{4} \gtrsim nT.$$

Initial estimation rate:

When the sparse rate is too small, then the above construction is not optimal, since we at least need to estimate the first matrix well without any sparse structures. Therefore, we consider we consider T copies of the same matrix. Note that the sparse constraint on the differences of the matrix is automatically satisfied when all matrices are the same. By constructing the following subset

$$\Xi_\epsilon = \{\Theta^{(w)} : \mathbf{U}_t^{(w)} = \mathbf{U}^w, \mathbf{V}_t^{(w)} = \mathbf{V}_0, \quad \forall t = 1, \dots, T, \mathbf{w} \in \Omega_M\}. \quad (12)$$

the KL divergence between any elements $\Theta \in \Xi_\epsilon$ and Θ^0 can be upper bounded:

$$D_{KL}(P_\Theta \| P_{\Theta^0}) \lesssim T(p-d-1)\|\mathbf{w}\|_2^2\epsilon^2 \leq Tn_0(p-d-1)\epsilon^2. \quad (13)$$

Let n_0 be the largest possible integer less than or equal to $(n - d - 1)$, then it suffices to let

$$T(n - d - 1)(p - d - 1)\epsilon^2 \lesssim n - d - 1.$$

Therefore, we can choose $\epsilon = \sqrt{1/((p - d - 1)T)}$. Then we have

$$d^2(\Theta^{(w_1)}, \Theta^{(w_2)}) \gtrsim Tn_0(p - d + 1)\epsilon^2 \gtrsim n.$$

Finally, based on Markov's inequality, by combining all the above cases, we have

$$\inf_{\hat{\Theta}} \sup_{\Theta \in \text{DSF}(s_u, s_v)} \mathbf{E}_{\Theta} \left[\frac{1}{Tnp} \sum_{t=1}^T \|\hat{U}_t \hat{V}_t' - U_t^* V_t^{*'}\|_F^2 \right] \gtrsim \frac{1}{npT} \left\{ s_u \log \left(\frac{Tn}{s_u} \right) + n \right\}. \quad (14)$$

By the alternating technique: fixing \mathcal{U} and construct similar hypothesis set for \mathcal{V} , we can also obtain the other rate of the lower bound

$$\inf_{\hat{\Theta}} \sup_{\Theta \in \text{DSF}(s_u, s_v)} \mathbf{E}_{\Theta} \left[\frac{1}{Tnp} \sum_{t=1}^T \|\hat{U}_t \hat{V}_t' - U_t^* V_t^{*'}\|_F^2 \right] \gtrsim \frac{1}{npT} \left\{ s_v \log \left(\frac{Tp}{s_v} \right) + p \right\}. \quad (15)$$

Then the final conclusion is obtained.

7.5.2 Symmetric case

In the symmetric case, we adopt a different hypothesis construction. Let $\Omega_M = \{\mathbf{w}^{(1)}, \dots, \mathbf{w}^{(M)}\} \subset \{0, 1\}^{(n-d+1)/2}$ constructed based on the above Lemma 7.1 (the construction holds under $n - d + 1 \geq 8$). For each \mathbf{w} , we can construct a $n \times d$ matrix as follows:

$$\mathbf{U}^w = \begin{bmatrix} \mathbf{u}^w & \mathbf{0} \\ \mathbf{0} & \mathbf{I}_{d-1} \end{bmatrix} \quad \text{with} \quad \mathbf{u}^w = \begin{bmatrix} 1 \\ \vdots \\ 1 \\ \epsilon \mathbf{w} \end{bmatrix} \in \mathbb{R}^{n-d+1}, w \in \Omega_M$$

where the first $(n - d + 1)/2$ components for \mathbf{u}^w are all ones.

The effect of this construction is that: for different $\mathbf{w}_1, \mathbf{w}_2 \in \Omega_M$, since $n_0/2 \leq \|\mathbf{w}_1 - \mathbf{w}_2\|_0 \leq 2n_0$ and $\|\mathbf{U}^w\|_F \leq \sqrt{n}$, we have

$$\begin{aligned} d_0(\mathbf{U}^{w_1}, \mathbf{U}^{w_2}) &\leq \|\mathbf{U}^{w_1} \mathbf{U}'^{w_1} - \mathbf{U}^{w_2} \mathbf{U}'^{w_2}\|_F \leq \|\mathbf{U}^{w_1} (\mathbf{U}'^{w_1} - \mathbf{U}'^{w_2})\|_F + \|(\mathbf{U}^{w_1} - \mathbf{U}^{w_2}) \mathbf{U}'^{w_2}\|_F \\ &\leq 2\sqrt{n} \|\mathbf{U}^{w_1} - \mathbf{U}^{w_2}\|_F = 2\sqrt{n} \|\mathbf{u}^{w_1} - \mathbf{u}^{w_2}\|_2 \leq 2\sqrt{2nn_0}\epsilon. \end{aligned}$$

In addition, consider $A := \{i + (n - d + 1)/2 : w_{1i} \neq 0\}$, $B := \{j + (n - d + 1)/2 : w_{2j} \neq 0\}$, $C := A \cap B$, where w_{1i}, w_{2j} are i and j th component of w_1 and w_2 . We have $|C| \leq n_0/2$, $|A - C| \geq n_0/2$ and $|B - C| \geq n_0/2$.

$$d_0^2(\mathbf{U}^{w_1}, \mathbf{U}^{w_2}) = \sum_{i \neq j}^{n-d+1} (u_i^{w_1} u_j^{w_1} - u_i^{w_2} u_j^{w_2})^2.$$

By only considering the sum for $i \in \{1, \dots, (n-d+1)/2\}, j \in A-C$ where $u_i^{w_1} = u_i^{w_2} = 1$, $u_j^{w_1} = \epsilon, u_j^{w_2} = 0$ and $i \neq j$, we have

$$d_0^2(\mathbf{U}^{w_1}, \mathbf{U}^{w_2}) \geq \sum_{i=1}^{(n-d+1)/2} \sum_{j \in A-C} (\epsilon w_{1j} - \epsilon w_{2j})^2 \geq \frac{n_0(n-d+1)}{4} \epsilon^2.$$

Let

$$\mathbf{U}^0 = \begin{bmatrix} \mathbf{0} & \mathbf{0} \\ \mathbf{0} & \mathbf{I}_{d-1} \end{bmatrix} \quad \text{with} \quad \mathbf{v}^{w_0} = \begin{bmatrix} 1 \\ \vdots \\ 1 \\ \mathbf{w}_0 \end{bmatrix} \in \mathbb{R}^{n-d+1}$$

and $\mathcal{U}^0 = [\mathbf{U}^0, \dots, \mathbf{U}^0]$. We need the above Varshamov-Gilbert Bound 7.1 again to introduce another binary coding: Let $\Omega_r = \{\phi^{(1)}, \dots, \phi^{(M_0)}\} \subset \{0, 1\}^T$, such that $\|\phi^{(i)}\|_0 = t_0$ for all $1 \leq i \leq M_0$ and $\|\phi^{(i)} - \phi^{(j)}\|_0 \geq t_0/2$ for $0 \leq i < j \leq M_0$ with $\log M_0 \geq ct_0 \log(T/t_0)$ with $c \geq 0.233$.

Then we have the following construction:

$$\begin{aligned} \Xi_\epsilon &= \{\mathcal{U}^{(w, \phi)} : \\ &\quad \mathbf{U}_t^{(w, \phi)} = \mathbf{U}^{w^{(i)}}, \quad \text{if } \phi_t = 1, \\ &\quad \mathbf{U}_t^{(w, \phi)} = \mathbf{U}^0, \quad \text{if } \phi_t = 0, \\ &\quad \mathbf{w}^{(i)} \in \Omega_M, \forall i = 1, \dots, t_0, \mathbf{w}^{(i)} \text{ is chosen with replacement, } \phi \in \Omega_r\}, \end{aligned}$$

For example, when $\phi = (0, 1, 0, 1, 0, 1, \dots)$, $\mathbf{U}_1^{(w, \phi)}, \dots, \mathbf{U}_T^{(w, \phi)}$ is:

$$\mathbf{U}^0, \mathbf{U}^{w^{(1)}}, \mathbf{U}^0, \mathbf{U}^{w^{(2)}}, \mathbf{U}^0, \mathbf{U}^{w^{(3)}}, \dots$$

for $\mathcal{U}^a, \mathcal{U}^b \in \Xi_\epsilon$, we have

$$d^2(\mathcal{U}^a, \mathcal{U}^b) = \sum_{t=1}^T d_0^2(\mathbf{U}_t^a, \mathbf{U}_t^b) \geq \frac{t_0 n_0 (n-d+1)}{8} \epsilon^2.$$

We have $|\Xi_\epsilon| = M_0 M^{t_0}$.

In addition, the KL divergence between any elements $\mathcal{U} \in \Xi_\epsilon$ and \mathcal{U}^0 can be upper bounded:

$$D_{kl}(P_{\mathcal{U}} \| P_{\mathcal{U}^0}) \leq C_0 d^2(\mathcal{U}, \mathcal{V}) \leq 4C_0 t_0 n_0 \epsilon^2,$$

for some constant $C_0 > 0$ ($C_0 = 1$ for the binary case, $C_0 = 1/(2\sigma^2)$ for the Gaussian case).

Based on the construction, we have for $\mathcal{U} \in \Xi_\epsilon$, $\sum_{t=2}^T \mathbb{1}\{D\mathbf{u}_{it} \neq 0\} \leq 2t_0$ for $i = 1, \dots, n$ and $\sum_{i=1}^n \mathbb{1}\{D\mathbf{u}_{it} \neq 0\} \leq 2n_0$ for $t = 2, \dots, T$. Therefore we have

$$\sum_{i=1}^n \sum_{t=2}^T \mathbb{1}\{D\mathbf{u}_{it} \neq 0\} \leq 4t_0 n_0.$$

We use the following Lemma 7.2 to show final prove that the minimax rate holds:

Sparse rate ($s \leq T$):

When $s \leq T$. Denote $n_0 = 1$ and $t_0 = s/4$, which satisfies $4n_0t_0 \leq s$. Then it's enough to set

$$sn\epsilon^2 \leq \alpha cs \log(4T/s) + \alpha cs \log\left(\frac{n-d-1}{2}\right)/8$$

with $c = 0.233/C_0$.

By taking $\epsilon = c^* \sqrt{s \log(Tn/s)/n}$ for some constant $c^* > 0$ such that the above inequality is satisfied, we have

$$\frac{t_0 n_0 (n-d+1) \epsilon^2}{8} \gtrsim s \log(Tn/s).$$

Sparse rate ($s > T$):

First, suppose $(n-d-1)T/8 > s > T$, we assume s/T is an integer for simplicity since it doesn't affect the final rate.

Denote $n_0 = s/T$ and $t_0 = T/4$, which satisfies $4n_0t_0 \leq s$. Since $s/T \leq (n-d-1)/8$, the construction holds given. To adopt the above Lemma 7.2, it suffices to show

$$2C_0 sn\epsilon^2/4 \leq \alpha \log(M_0 M^{T/4}) = \alpha \log(|\Xi_\epsilon|),$$

with $\alpha < 1/8$. Then we need to set

$$sn\epsilon^2 \leq \alpha cT \log 4 + \alpha cs \log\left(\frac{(n-d-1)T}{2s}\right)/2$$

with $c = 0.233/C_0$.

By taking $\epsilon = c^* \sqrt{\log(nT/s)/n}$ for some constant $c^* > 0$ such that the above inequality is satisfied, we have

$$\frac{t_0 n_0 (n-d+1) \epsilon^2}{8} \gtrsim s \log(Tn/s).$$

Dense rate:

If $s \geq (n-d-1)T/8$, the difference between latent vectors is dense instead. Then we assign $n_0 = (n-d-1)/8$ and $t_0 = T/4$, which satisfies the constraint. In this case, we need to set

$$(n-d-1)T/32n\epsilon^2 \leq \alpha cT \log 4 + \alpha cT(n-d-1) \log 4/4$$

with $c = 0.233/C_0$.

By taking $\epsilon = c^* \sqrt{1/n}$ for some constant $c^* > 0$ such that the above inequality is satisfied, we have

$$\frac{t_0 n_0 (n-d+1) \epsilon^2}{8} \gtrsim nT.$$

Initial estimation rate:

When the sparse rate is too small, then the above construction is not optimal, since we at least need to estimate the first matrix well without any sparse structures. Therefore, we consider we consider T copies of the same matrix. Note that the sparse constraint on the differences of the matrix is automatically satisfied when all matrices are the same. By constructing the following subset

$$\Xi_\epsilon = \{\mathcal{U}^{(w)} : \mathbf{U}_t^{(w)} = \mathbf{U}^w, \quad \forall t = 1, \dots, T, \mathbf{w} \in \Omega_M\}. \quad (16)$$

the KL divergence between any elements $\mathcal{U} \in \Xi_\epsilon$ and \mathcal{U}^0 can be upper bounded:

$$D_{KL}(P_{\mathcal{U}} || P_{\mathcal{U}^0}) \leq C_0 d_0^2(\mathbf{U}_t, \mathbf{V}_t) \leq 4Tn(n-d-1)\epsilon^2. \quad (17)$$

Let n_0 be the largest possible value $(n-d-1)/8$, then it suffices to let

$$4Tn(n-d-1)\epsilon^2 \leq \frac{c(n-d-1)\log 4}{16} \leq \alpha \log(M).$$

Therefore, based on the above equation, we need to choose $\epsilon = \sqrt{1/(nT)}$. Then we have

$$\frac{t_0 n_0 (n-d+1)\epsilon^2}{8} \gtrsim n.$$

Finally, based on Markov's inequality, by combining all the above cases the final conclusion holds. □

7.6 Proof of Theorem 3.2

Denote the ϵ ball for KL divergence neighborhood centered at Θ^* as

$$B_n(\Theta^*; \epsilon) = \left\{ \Theta \in \Xi : \int p_{\Theta^*} \log\left(\frac{p_{\Theta^*}}{p_{\Theta}}\right) d\mu \leq npT\epsilon^2, \int p_{\Theta^*} \log^2\left(\frac{p_{\Theta^*}}{p_{\Theta}}\right) d\mu \leq npT\epsilon^2 \right\},$$

where μ is the Lebesgue measure.

Based on Assumption 1, we have $\max\{D_{KL}(p_{\Theta}, p_{\Theta^*}), V_2(p_{\Theta}, p_{\Theta^*})\} \lesssim \sum_{t=1}^T \|\mathbf{U}_t \mathbf{V}_t' - \mathbf{U}_t \mathbf{V}_t^{*'}\|_F^2$. Hence we only need to lower bound the prior probability of the set $E_0 := \{\sum_{i,j,t} (\mathbf{u}_{it}' \mathbf{v}_{jt} - \mathbf{u}_{it}^{*'} \mathbf{v}_{jt}^*)^2 \leq npT\epsilon^2\} \supset \{\max_{i,j,t} (\mathbf{u}_{it}' \mathbf{v}_{jt} - \mathbf{u}_{it}^{*'} \mathbf{v}_{jt}^*)^2 \leq \epsilon^2\}$. Given $i \neq j, t$ we have

$$\begin{aligned} |\mathbf{u}_{it}' \mathbf{v}_{jt} - \mathbf{u}_{it}^{*'} \mathbf{v}_{jt}^*| &\leq |(\mathbf{u}_{it}' - \mathbf{u}_{it}^{*'}) \mathbf{v}_{jt}^*| + |\mathbf{u}_{it}' (\mathbf{v}_{jt} - \mathbf{v}_{jt}^*)| = |(\mathbf{u}_{it}' - \mathbf{u}_{it}^{*'}) \mathbf{v}_{jt}^*| + |(\mathbf{u}_{it}' - \mathbf{u}_{it}^{*'} + \mathbf{u}_{it}^{*'}) (\mathbf{v}_{jt} - \mathbf{v}_{jt}^*)| \\ &\leq \|\mathbf{u}_{it} - \mathbf{u}_{it}^*\|_2 \|\mathbf{v}_{jt}^*\|_2 + \|\mathbf{v}_{jt} - \mathbf{v}_{jt}^*\|_2 \|\mathbf{u}_{it}^*\|_2 + \|\mathbf{u}_{it} - \mathbf{u}_{it}^*\|_2 \|\mathbf{v}_{jt} - \mathbf{v}_{jt}^*\|_2 \end{aligned}$$

Note that $\max\{\mathbf{u}_{it}^*, \mathbf{v}_{jt}^*\} \leq C$ for a constant C based on assumption. Then when $\epsilon = o(1)$, $\max_{it} \|\mathbf{u}_{it} - \mathbf{u}_{it}^*\|_2 \leq \epsilon/3C$ and $\max_{jt} \|\mathbf{v}_{jt} - \mathbf{v}_{jt}^*\|_2 \leq \epsilon/3C$, we have

$$\max_{i,j,t} |\mathbf{u}_{it}' \mathbf{v}_{jt} - \mathbf{u}_{it}'^* \mathbf{v}_{jt}^*| \leq \frac{2\epsilon}{3} + \frac{\epsilon^2}{9C^2} \leq \epsilon,$$

for large enough n, p, T . We first show the prior concentration for $\max_{it} \|\mathbf{u}_{it} - \mathbf{u}_{it}^*\|_2 \leq \epsilon/3C$, the prior concentration for $\max_{jt} \|\mathbf{v}_{jt} - \mathbf{v}_{jt}^*\|_2 \leq \epsilon/3C$ will be similarly derived.

Let $\epsilon_u = \sqrt{(s_u + n) \log(npT)/(npT)}$, then $npT\epsilon_u^2 = (s_u + n) \log(npT)$, suppose for subjects i the sparsity is s_{ui} such that $\sum_{i=1}^n s_{ui} = s_u$.

Denote $E_0 = \{\max_{it} \|\mathbf{u}_{it} - \mathbf{u}_{it}^*\|_2 \leq C_0 \epsilon/3C\}$ for some large enough constant $C_0 > 0$, $E_1 = \{\max_{i,j,t} |(U_{ijt} - U_{ij1}) - (U_{ijt}^* - U_{ij1}^*)| \leq \epsilon_{ui}\}$, $E_2 = \{\max_{i,j} |U_{ij1} - U_{ij1}^*| \leq \epsilon_u\}$ with $\epsilon_{ui} = \sqrt{(s_{ui} + 1) \log(npT)/(3C\sqrt{d}npT)}$. Note that $\sum_{i=1}^n \epsilon_{ui}^2 \lesssim \epsilon_u^2$, so we have $E_1 \cap E_2 \subset E_0$ as long as C_0 is a large enough constant, which implies that

$$\Pi(E_0) \geq \Pi(E_1) \Pi(E_2) = \prod_{i,j} \Pi\left(\sup_{t \geq 2} |\tilde{U}_{ijt} - \tilde{U}_{ijt}^*| \leq \epsilon_{ui}\right) \prod_{i,j} \Pi(|U_{ij1} - U_{ij1}^*| \leq \epsilon_u),$$

where $\tilde{U}_{ijt} = U_{ijt} - U_{ij1}$ for all i, j, t . Note that we have by triangular inequality:

$$|\tilde{U}_{ijt} - \tilde{U}_{ijt}^*| \leq \sum_{t_0=2}^t |\tilde{U}_{ijt_0} - \tilde{U}_{ij(t_0-1)} - (\tilde{U}_{ijt_0}^* - \tilde{U}_{ij(t_0-1)}^*)|.$$

Therefore, based on Lemma 7.4 and $\epsilon_{ui} = O(\sqrt{\max\{s_{ui}, 1\} \log(npT)/(npT)})$, and the choice of τ_u , we have

$$\begin{aligned} & \Pi\left(\sup_{t \geq 2} |\tilde{U}_{ijt} - \tilde{U}_{ijt}^*| \leq \epsilon_{ui}\right) \\ & \geq \Pi\left(\sum_{t=2}^T |\tilde{U}_{ijt} - \tilde{U}_{ij(t-1)} - (\tilde{U}_{ijt}^* - \tilde{U}_{ij(t-1)}^*)| \leq C_2 \sqrt{\frac{\max\{s_{ui}, 1\} \log(npT)}{npT}}\right) \\ & \gtrsim e^{-K(s_i+1) \log(npT)}, \end{aligned}$$

for some constant $C_2, K > 0$, $i = 1, \dots, n$ and $j = 1, \dots, d$, since each $\tilde{U}_{ijt} - \tilde{U}_{ij(t-1)}$ is assigned with a component of the shrinkage prior. This implies that

$$\Pi(E_1) \gtrsim e^{-K(s_u+n) \log(npT)}.$$

Let $\sigma_0^* = 1$, we consider the event on the initial variance $E_3 = \{|\sigma_{0i}^2 - \sigma_0^{*2}| \leq \sigma_0^{*2}/2\}$. Note that the density of Inverse-Gamma($a_{\sigma_0}, b_{\sigma_0}$) is lower bounded by a constant within the constrained space $[\sigma_0^{*2}/2, 3\sigma_0^{*2}/2]$. Therefore we have the prior concentration:

$$\Pi(E_3) = \prod_{i=1}^n \Pi(|\sigma_{0i}^2 - \sigma_0^{*2}| \leq \sigma_0^{*2}/2) \gtrsim e^{-K_2 n},$$

for some constant $K_2 > 0$.

Then for the initial error concentration $\Pi(E_2)$, by the mean-zero Gaussian of U_{ij1} for all i, j , we have the concentration:

$$\begin{aligned}\Pi(E_2) &= \Pi(E_2 \mid E_3)\Pi(E_3) = \prod_{i,j} \Pi(|U_{ij1} - U_{ij1}^*| \leq \epsilon_u \mid E_3) \Pi(E_3) \\ &\gtrsim \frac{1}{(\sqrt{2\pi}\sigma_0^*/\sqrt{2})^{nd}} \exp\left(-\sum_{i,j} \frac{U_{ij1}^{*2}}{2\sigma_0^{*2}}\right) (2\epsilon_u)^{nd} e^{-K_2 n} \\ &\gtrsim \exp\left[-K_3 \left\{\frac{\|\mathbf{U}_1^*\|_F^2}{2\sigma_0^{*2}} + nd + nd \log\left(\frac{1}{\epsilon_u}\right)\right\}\right].\end{aligned}\quad (18)$$

for some constant $K_3 > 0$. Note that σ_0^* is a constant and $\|\mathbf{U}_1^*\|_F^2 = O(n)$. We have $\log \Pi(E_2) \gtrsim -n \log(1/\epsilon_u)$ and $\log \Pi(E_0) \gtrsim -(s_u + n) \log(1/\epsilon_u)$.

Similarly, by the same technique, we can show that $\log \Pi(\max_{jt} \|\mathbf{v}_{jt} - \mathbf{v}_{jt}^*\|_2 \leq \epsilon_v) \gtrsim -(s_v + p) \log(1/\epsilon_v)$ for $\epsilon_v = \sqrt{(s_v + p) \log(npT)/(npT)}$. Finally, by choosing $\epsilon_{n,p,T} = \sqrt{\epsilon_u^2 + \epsilon_v^2}$, we have

$$\log \Pi(\max_{it} \|\mathbf{u}_{it} - \mathbf{u}_{it}^*\|_2 \leq \epsilon_{n,p,T}, \max_{jt} \|\mathbf{v}_{jt} - \mathbf{v}_{jt}^*\|_2 \leq \epsilon_{n,p,T}) \gtrsim -(s_u + s_v + n + p) \log(npT).$$

Note that for the symmetric case, the prior concentration still holds by only consider the concentration for \mathcal{U} : $\log \Pi(\max_{it} \|\mathbf{u}_{it} - \mathbf{u}_{it}^*\|_2 \leq \epsilon_{n,p,T}) \gtrsim -(s_u + n) \log(n^2T)$.

Finally, as shown in Theorem 3.2 in [Bhattacharya et al. \(2019\)](#), under the condition that

$$\Pi(B_n(\Theta^*; \epsilon_{n,p,T})) \geq e^{-Tnp\epsilon_{n,p,T}^2},$$

we can obtain the convergence of the α -divergence at the rate:

$$D_\alpha(p_\Theta, p_{\Theta^*}) = \frac{1}{\alpha - 1} \log \int (p_{\Theta^*})^\alpha (p_\Theta)^{1-\alpha} d\mu.$$

Therefore, the conclusion holds given the α -divergence is lower bounded by the loss function under Assumption 2.

7.7 Proof of Corollary 3.3

We first show that the static rate can be achieved marginally under the same prior for any time point. Given a time point t , the goal is to show the rate of estimating $\|\hat{\mathbf{U}}_t \hat{\mathbf{U}}_t' - \mathbf{U}_t^* \mathbf{U}_t^{*'}\|_F^2$ under the proposed prior. Note that the prior for each component of \mathbf{u}_{it} is $\mathcal{N}(0, \sigma_{it}^2)$ conditional on $\sigma_{0i}, \lambda_{it_0}, t_0 = 1, \dots, t$, with $\sigma_{it}^2 = \sigma_{0i}^2 + \sum_{t_0=1}^{t-1} \lambda_{it_0}^2 \tau_u^2$. We can consider the above prior in estimation of t_0 copies of \mathbf{U}_t^* : for time point $1, \dots, t$, the true latent matrices are $\mathbf{U}_t^*, \mathbf{U}_t^*, \dots, \mathbf{U}_t^*$, where the sparsity of the transitions is zero. Note that the prior concentration of the proposed prior on the truth is $(n + s) \log(nT)$, while now $s =$

0. This implies that the prior concentration for $\|\hat{\mathbf{U}}_t \hat{\mathbf{U}}_t' - \mathbf{U}_t^* \mathbf{U}_t^{*'}\|_F^2$ is $n \log(nT)$, by the same argument with proof of the dynamic rate, we have for large enough n , we have $\|\hat{\mathbf{U}}_t \hat{\mathbf{U}}_t' - \mathbf{U}_t^* \mathbf{U}_t^{*'}\|_F^2 \lesssim n \log(nT)$ for any t .

To prove the final conclusion, we start with $t = 1$, which corresponds to the truth $\mathbf{U}_1^*, \mathbf{U}_2^*$. For any $t_0 = 1, \dots, T$, we denote

$$\mathbf{O}_{t_0} = \operatorname{argmin}_{\mathbf{O} \in \mathbb{O}^{d \times d}} \|\hat{\mathbf{U}}_{t_0}^o - \mathbf{U}_{t_0}^* \mathbf{O}\|_F.$$

First, note that $\hat{\mathbf{U}}_1^o = \hat{\mathbf{U}}_1$, consider the common matrix \mathbf{O}_1 , we have

$$\begin{aligned} \|\hat{\mathbf{U}}_2^o \hat{\mathbf{O}}_{21} - \mathbf{U}_2^* \mathbf{O}_1\|_F &\leq \|\hat{\mathbf{U}}_2^o \hat{\mathbf{O}}_{21} - \hat{\mathbf{U}}_1^o\|_F + \|\hat{\mathbf{U}}_1^o - \mathbf{U}_1^* \mathbf{O}_1\|_F + \|\mathbf{U}_1^* \mathbf{O}_1 - \mathbf{U}_2^* \mathbf{O}_1\|_F \\ &\leq \|\hat{\mathbf{U}}_2^o \hat{\mathbf{O}}_{21} - \hat{\mathbf{U}}_1^o\|_F + \|\hat{\mathbf{U}}_1^o - \mathbf{U}_1^* \mathbf{O}_1\|_F + \|\mathbf{U}_1^* - \mathbf{U}_2^*\|_F, \end{aligned}$$

and

$$\begin{aligned} \|\hat{\mathbf{U}}_2^o \hat{\mathbf{O}}_{21} - \hat{\mathbf{U}}_1^o\|_F &\leq \|\hat{\mathbf{U}}_2^o \mathbf{O}_2' - \hat{\mathbf{U}}_1^o \mathbf{O}_1'\|_F \\ &\leq \|\hat{\mathbf{U}}_2^o \mathbf{O}_2' - \mathbf{U}_2^*\|_F + \|\mathbf{U}_2^* - \mathbf{U}_1^*\|_F + \|\hat{\mathbf{U}}_1^o \mathbf{O}_1' - \mathbf{U}_1^*\|_F \\ &= \|\hat{\mathbf{U}}_2^o - \mathbf{U}_2^* \mathbf{O}_2\|_F + \|\mathbf{U}_2^* - \mathbf{U}_1^*\|_F + \|\hat{\mathbf{U}}_1^o - \mathbf{U}_1^* \mathbf{O}_1\|_F. \end{aligned}$$

The above two inequalities imply that

$$\|\hat{\mathbf{U}}_2^o \hat{\mathbf{O}}_{21} - \mathbf{U}_2^* \mathbf{O}_1\|_F \leq 2\|\hat{\mathbf{U}}_1^o - \mathbf{U}_1^* \mathbf{O}_1\|_F + \|\hat{\mathbf{U}}_2^o - \mathbf{U}_2^* \mathbf{O}_2\|_F + 2\|\mathbf{U}_2^* - \mathbf{U}_1^*\|_F.$$

Therefore, similarly, for $k \geq 3$, we have

$$\|\hat{\mathbf{U}}_k^o \hat{\mathbf{O}}_{k1} - \mathbf{U}_k^* \mathbf{O}_1\|_F \leq \|\hat{\mathbf{U}}_k^o - \mathbf{U}_k^* \mathbf{O}_k\|_F + 2\|\mathbf{U}_k^* - \mathbf{U}_1^*\|_F + 2\|\hat{\mathbf{U}}_1^o - \mathbf{U}_1^* \mathbf{O}_1\|_F,$$

which implies that

$$\|\hat{\mathbf{U}}_k^o \hat{\mathbf{O}}_{k1} - \mathbf{U}_k^* \mathbf{O}_1\|_F^2 \leq 2\|\hat{\mathbf{U}}_k^o - \mathbf{U}_k^* \mathbf{O}_k\|_F^2 + 16\|\mathbf{U}_k^* - \mathbf{U}_1^*\|_F^2 + 16\|\hat{\mathbf{U}}_1^o - \mathbf{U}_1^* \mathbf{O}_1\|_F^2.$$

Therefore, by induction, we have

$$\sum_{k_0=1}^k \|\hat{\mathbf{U}}_{k_0}^o \hat{\mathbf{O}}_{k_0 1} - \mathbf{U}_{k_0}^* \mathbf{O}_1\|_F^2 \leq 2 \sum_{k_0=1}^k \|\hat{\mathbf{U}}_{k_0}^o - \mathbf{U}_{k_0}^* \mathbf{O}_{k_0}\|_F^2 + 16 \sum_{k_0=1}^k \|\mathbf{U}_{k_0}^* - \mathbf{U}_1^*\|_F^2 + 16k \|\hat{\mathbf{U}}_1^o - \mathbf{U}_1^* \mathbf{O}_1\|_F^2.$$

For large enough n , we have $\|\hat{\mathbf{U}}_t \hat{\mathbf{U}}_t' - \mathbf{U}_t^* \mathbf{U}_t^{*'}\|_F$. By the eigenvalue condition, we have $\|\mathbf{U}_t^{*\dagger}\| \lesssim 1/\sqrt{n}$ where $\mathbf{U}_t^{*\dagger}$ is the psedo-inverse of \mathbf{U}_t^* . The above two conclusion implies that $\|\mathbf{U}_t^{*\dagger}\| \sqrt{\|\hat{\mathbf{U}}_t \hat{\mathbf{U}}_t' - \mathbf{U}_t^* \mathbf{U}_t^{*'}\|_F} \leq 1/2$ for large enough n . Therefore, by Lemma 7.5, we have:

$$\|\hat{\mathbf{U}}_t^o - \mathbf{U}_t^* \mathbf{O}_t\|_F \lesssim \|\hat{\mathbf{U}}_t \mathbf{U}_t' - \mathbf{U}_t^* \mathbf{U}_t^{*'}\|_F / \sqrt{n} \lesssim \sqrt{\log nT}.$$

For the rest of the windows (e.g., $\mathbf{U}_{k+1}^*, \dots, \mathbf{U}_{2k-1}^*$), the proof follows the same technique, with the common orthogonal transformation \mathbf{O}_k . Then when the average error is considered, note that

$$\begin{aligned} & \sum_{t=1}^{\bar{t}} \sum_{k_0=1}^k \|\hat{\mathbf{U}}_{(t-1)k+k_0}^o - \mathbf{U}_{(t-1)k+k_0}^* \mathbf{O}_{(t-1)k+1}\|_F^2 \\ & \lesssim \sum_{t=1}^{\bar{t}} \sum_{k_0=1}^k \|\hat{\mathbf{U}}_{(t-1)k+k_0}^o - \mathbf{U}_{(t-1)k+k_0}^* \mathbf{O}_{(t-1)k+k_0}\|_F^2 \\ & + \sum_{t=1}^{\bar{t}} \sum_{k_0=1}^k \|\mathbf{U}_{(t-1)k+k_0}^* - \mathbf{U}_{(t-1)k+1}^*\|_F^2 + \sum_{t=1}^{\bar{t}} k \|\hat{\mathbf{U}}_{(t-1)k+1}^o - \mathbf{U}_{(t-1)k+1}^* \mathbf{O}_{(t-1)k+1}\|_F^2. \end{aligned}$$

First, by the estimation error rate, we have

$$\begin{aligned} & \sum_{t=1}^{\bar{t}} k \|\hat{\mathbf{U}}_{(t-1)k+1}^o - \mathbf{U}_{(t-1)k+1}^* \mathbf{O}_{(t-1)k+1}\|_F^2 \\ & \lesssim \min\left\{\sum_{t=1}^T k \|\hat{\mathbf{U}}_t - \mathbf{U}_t^* \mathbf{O}_t\|_F^2, T \log(nT)\right\} \lesssim \min\{k(s+n) \log(nT)/n, T \log(nT)\}; \end{aligned}$$

and

$$\begin{aligned} & \sum_{t=1}^{\bar{t}} \sum_{k_0=1}^k \|\hat{\mathbf{U}}_{(t-1)k+k_0}^o - \mathbf{U}_{(t-1)k+k_0}^* \mathbf{O}_{(t-1)k+k_0}\|_F^2 \\ & \lesssim \sum_{t=1}^T 2 \|\hat{\mathbf{U}}_t - \mathbf{U}_t^* \mathbf{O}_t\|_F^2 \lesssim (s+n) \log(nT)/n. \end{aligned}$$

Suppose the true transitions are $s_1, \dots, s_{\bar{t}}, t = 1, \dots, \bar{t}$ in each window, then $\sum_{t=1}^{\bar{t}} s_t = s$, then we have for any $t, k, k_0 > 1$, $\|\mathbf{U}_{(t-1)k+k_0}^* - \mathbf{U}_{(t-1)k+1}^*\|_F \lesssim \min\{\sqrt{s_t k}, \sqrt{s}, \sqrt{n}\}$. Therefore, we have

$$\sum_{t=1}^{\bar{t}} \sum_{k_0=1}^k \|\mathbf{U}_{(t-1)k+k_0}^* - \mathbf{U}_{(t-1)k+1}^*\|_F^2 \lesssim \min\{sk(k-1), Tn, sT\}.$$

Therefore, the final conclusion holds by aggregating the corresponding three terms.

7.8 An improved rate for Corollary 3.3

The rate in Corollary 3.3 is not optimal in some special cases. Consider that there is only one node change $O(T)$ times with $T > n$, then the best rate of k could only approach $O(\sqrt{n}) \leq O(\sqrt{T})$. This does not match our intuition that when almost all nodes do not change, it should be no problem to compare all latent positions across all time. To handle this case, we consider the following more stringent assumption:

Assumption 4 (Active nodes constraint). *There is a $s_{0,k} = o(n)$, such that*

$$\max_{k_0=1}^k \max_{t=1}^T \|\mathbf{U}_{(t-1)k+k_0}^* - \mathbf{U}_{(t-1)k+1}^*\|_{2,0} \leq s_{0,k}. \quad (19)$$

The Assumption 4 assumes that within a window for $k_0 = 1, \dots, k$, only at most $2s_{0,k}$ of n nodes transit over time, which are therefore considered as ‘active nodes’, while the rest of nodes remain static. However, the active nodes can transit over all time points.

Corollary 7.3. *Under the assumptions in 3.3, if we further assume that Assumption 4 holds, then we have*

$$\inf_{\bar{\mathbf{O}}_{t,k} \in \mathbb{O}^{d \times d}} \sum_{k_0=1}^k \|\hat{\mathbf{U}}_{(t-1)k+k_0}^o - \mathbf{U}_{(t-1)k+k_0}^* \bar{\mathbf{O}}_{t,k}\|_F^2 \lesssim k \log nT + s_{0,k}(k-1),$$

and the average error for all windows satisfies

$$\begin{aligned} \frac{1}{nT} \sum_{t=0}^{\bar{t}-1} \inf_{\bar{\mathbf{O}}_{t,k} \in \mathbb{O}^{d \times d}} \sum_{k_0=1}^k \|\hat{\mathbf{U}}_{(t-1)k+k_0}^o - \mathbf{U}_{(t-1)k+k_0}^* \bar{\mathbf{O}}_{t,k}\|_F^2 &\lesssim \frac{(s+n) \log(nT)}{n^2 T} \\ &+ \min \left\{ \frac{k(s+n) \log(nT)}{n^2 T}, \frac{\log(nT)}{n} \right\} + \min \left\{ \frac{sk(k-1)}{nT}, \frac{s_{0,k}}{n} \right\}. \end{aligned}$$

According to Corollary 3.3, as long as $s_{0,k} = o(n)$ (which is possible when $s = o(nT)$, therefore improved upon Theorem 3.3), then one can compare all the latent space for time points of length $k = O(T)$ simultaneously, which can be intuitively explained that when the majority of nodes do not move across all time, there is no need to adjust the axis within all the time period.

Proof. Under Assumption 7.3, we can improve the following bound: for any $t, k, k_0 > 1$, $\|\mathbf{X}_{(t-1)k+k_0}^* - \mathbf{X}_{(t-1)k+1}^*\|_F \lesssim \sqrt{s_t k}, \sqrt{s_{0,k}}$ in the final step in the proof in subsection ???. Therefore, we have

$$\sum_{t=0}^{\bar{t}} \sum_{k_0=1}^k \|\mathbf{X}_{(t-1)k+k_0}^* - \mathbf{X}_{(t-1)k+1}^*\|_F^2 \lesssim \min\{sk(k-1), s_{0,k}T\},$$

and the rest follows similarly. □

7.9 Proof of Theorem 3.4

For any $t = 1, \dots, T$, denote

$$\mathbf{O}_t = \operatorname{argmin}_{\mathbf{O} \in \mathbb{O}^{d \times d}} \|\hat{\mathbf{U}}_t - \mathbf{U}_t^* \mathbf{O}\|_F.$$

Note that $\mathbf{U}_t^* \mathbf{O}$ has the same cluster configuration with \mathbf{U}_t^* . Note that for large enough n , we have $\|\hat{\mathbf{U}}_t \hat{\mathbf{U}}_t' - \mathbf{U}_t^* \mathbf{U}_t^{*'}\|_F \lesssim \sqrt{n \log n T}$ by the posterior concentration for the static latent space model. By assumption 2, we have $\|\mathbf{U}_t^{*\dagger}\| \lesssim 1/\sqrt{n}$ where $\mathbf{U}_t^{*\dagger}$ is the psedo-inverse of \mathbf{U}_t^* . The above two conclusion implies that $\|\mathbf{U}_t^{*\dagger}\| \sqrt{\|\hat{\mathbf{U}}_t \hat{\mathbf{U}}_t' - \mathbf{U}_t^* \mathbf{U}_t^{*'}\|_F} \leq 1/2$ for large enough n . Therefore, by Lemma 7.5, we have:

$$\|\hat{\mathbf{U}}_t - \mathbf{U}_t^* \mathbf{O}_t\|_F \lesssim \|\hat{\mathbf{U}}_t \hat{\mathbf{U}}_t' - \mathbf{U}_t^* \mathbf{U}_t^{*'}\|_F / \sqrt{n} \lesssim \sqrt{\log n T}.$$

Note that the smallest cluster size is greater than $16\|\hat{\mathbf{U}}_t - \mathbf{U}_t^* \mathbf{O}_t\|_F^2 / \delta^2$. By lemma 7.6, the above bounds implies that by applying K_t means on $\hat{\mathbf{U}}_t$ to obtain $\hat{\mathbf{\Xi}}_t$, we have

$$L(\hat{\mathbf{\Xi}}_t, \mathbf{\Xi}_t) \leq 16\|\hat{\mathbf{U}}_t - \mathbf{U}_t^* \mathbf{O}_t\|_F^2 / \delta^2.$$

The above two inequalities lead to

$$\frac{\sum_{t=1}^T L(\hat{\mathbf{\Xi}}_t, \mathbf{\Xi}_t)}{T} \lesssim \frac{\sum_{t=1}^T \|\hat{\mathbf{U}}_t \hat{\mathbf{U}}_t' - \mathbf{U}_t^* \mathbf{U}_t^{*'}\|_F^2}{nT\delta^2} \lesssim \frac{(s+n) \log(nT)}{nT\delta^2}.$$

Therefore, the final conclusion holds.

7.10 Auxiliary Lemmas

Consider the prior concentration for dynamic networks with sparsity on the differences between two consecutive vectors of the same subject:

$$\begin{aligned} \lambda_t &\sim \text{Ca}^+(0, 1), \quad t = 1, \dots, T, \quad \tau \sim g \\ \beta_t &\sim \mathcal{N}(0, \lambda_t^2 \tau^2), \quad t = 1, \dots, T. \end{aligned} \tag{20}$$

In the following Lemma, we reformulate the form of prior concentration for shrinkage prior with additional variable n to fit the network and factor problems. Note that the additional variable n here stands for np for factor models and n^2 for network models.

Lemma 7.4 (ℓ_1 concentration for proposed shrinkage prior with additional variable n). *Suppose $\boldsymbol{\beta}^* \in \mathbb{R}^T$ with $S = \{j : \beta_j^* \neq 0\}$ and $|S| \leq s$, $1 \leq s \leq T$. Denote $\delta = \sqrt{s \log(nT)/(nT)}$ with $\log T = o(n)$, $n \geq 1$ and $\max_{t=1}^T |\beta_t| = O(n^\alpha T^\alpha)$ for some constant $\alpha > 0$. Under the above shrinkage prior (20) with g satisfying the following property:*

$$\log \{g(\tau^* < \tau < 2\tau^*)\} \gtrsim -s_i \log(nT), \quad \text{with} \quad \tau^* = \frac{s^{\frac{1}{2}} (\log(nT))^{\frac{1}{2}}}{n^{\frac{3}{2}} T^{\frac{5}{2}}}. \tag{21}$$

then for some constant $c_0 > 0$, we have

$$\Pi(\|\boldsymbol{\beta} - \boldsymbol{\beta}^*\|_1 \leq \delta) \geq e^{-Ks \log(nT)}, \tag{22}$$

where $K > 0$ is a constant.

Proof. $\log T = o(n)$ guarantees $\delta = o(1)$ for any $s = 1, \dots, T$.

First, we have

$$Pr(\|\boldsymbol{\beta} - \boldsymbol{\beta}^*\|_1 < \delta) \geq \prod_{j \in S} Pr(|\beta_j - \beta_j^*| < \frac{\delta}{2s}) \prod_{j \in S^c} Pr(|\beta_j - \beta_j^*| < \frac{\delta}{2T}),$$

Denote

$$\tau^* = \frac{s^{\frac{1}{2}}(\log(nT))^{\frac{1}{2}}}{n^{\frac{3}{2}}T^{\frac{5}{2}}}, \quad (23)$$

and consider the event $E_\tau = \{\tau : \tau \in [\tau^*, 2\tau^*]\}$.

For the non-signal part. For $j \in S^c$, by the Chernoff bound for a Gaussian random variable, we have

$$Pr(|\beta_j| > \frac{\delta}{2T} \mid \lambda_j, \tau) \leq 2e^{-\delta^2/(8T^2\lambda_j^2\tau^2)}.$$

Then we have

$$\begin{aligned} Pr(|\beta_j| < \frac{\delta}{2T} \mid \tau) &\geq \int_{\lambda_j} \left\{1 - 2e^{-\delta^2/(8T^2\lambda_j^2\tau^2)}\right\} f(\lambda_j) d\lambda_j \\ &= 1 - \int_{\lambda_j} 2e^{-\delta^2/(8T^2\lambda_j^2\tau^2)} f(\lambda_j) d\lambda_j, \end{aligned}$$

with $f(\lambda_j) = 1/(1 + \lambda_j^2) < \lambda_j^{-2}$. Then, we have

$$\begin{aligned} \int_{\lambda_j} 2e^{-\delta^2/(8T^2\lambda_j^2\tau^2)} f(\lambda_j) d\lambda_j &< 2 \int_{\lambda_j} e^{-\delta^2/(8T^2\lambda_j^2\tau^2)} \lambda_j^{-2} d\lambda_j \\ &= 2 \frac{\Gamma(1/2)}{\{\delta^2/(8T^2\tau^2)\}^{1/2}} \\ &= C \frac{T\tau}{\sqrt{s \log(nT)/(nT)}} \\ &\leq C' \frac{1}{nT}, \end{aligned}$$

where in the final step we use $\tau < 2\tau^*$.

Moreover, for the signal part, let $\delta_0 = \delta/(2s)$, we have

$$\begin{aligned}
Pr(|\beta_j - \beta_j^*| < \delta_0 \mid \tau) &= \int_{\lambda_j} \int_{|\beta_j - \beta_j^*| < \delta_0} \left(\frac{2}{\pi^3}\right)^{1/2} \exp\{-\beta_j^2/(2\lambda_j^2\tau^2)\} \frac{1}{\lambda_j\tau(1+\lambda_j^2)} d\lambda_j d\beta_j \\
&\geq \left(\frac{2}{\pi^3}\right)^{1/2} \int_{|\beta_j - \beta_j^*| < \delta_0} \int_{n^\alpha T^\alpha/\tau^*}^{2n^\alpha T^\alpha/\tau^*} \frac{1}{\sqrt{2\pi}} \exp\{-\beta_j^2/(2\lambda_j^2\tau^2)\} \frac{1}{\lambda_j\tau(1+\lambda_j^2)} d\lambda_j d\beta_j \\
&\stackrel{(i)}{\geq} \left(\frac{2}{\pi^3}\right)^{1/2} \int_{|\beta_j - \beta_j^*| < \delta_0} \exp\{-\beta_j^2/(4n^{2\alpha}T^{2\alpha})\} \int_{n^\alpha T^\alpha/\tau^*}^{n^\alpha T^\alpha/\tau^*} \frac{1}{4n^\alpha T^\alpha(1+\lambda_j^2)} d\lambda_j d\beta_j \\
&\geq \left(\frac{2}{\pi^3}\right)^{1/2} \frac{\tau}{2(4n^{2\alpha}T^{2\alpha} + \tau^2)} \int_{|\beta_j - \beta_j^*| < \delta_0} \exp\{-\beta_j^2/(4n^{2\alpha}T^{2\alpha})\} d\beta_j \\
&\stackrel{(ii)}{\geq} K\delta_0\tau^*n^{-2\alpha}T^{-2\alpha} \\
&\geq K'\frac{\sqrt{\log(nT)}}{\sqrt{nTs}}n^{-2\alpha}T^{-2\alpha}\frac{s^{\frac{1}{2}}(\log(nT))^{\frac{1}{2}}}{n^{\frac{3}{2}}T^{\frac{5}{2}}} \stackrel{(iii)}{\geq} K''(nT)^{-M}
\end{aligned}$$

where (i) holds based on $n^\alpha T^\alpha < \tau\lambda_j < 4n^\alpha T^\alpha$; (ii) is due to $\tau < 1$ and $\max_t(|\beta_t|) = O(n^\alpha T^\alpha)$; (iii) is because $s < p$; $M, K, K', K'' > 0$ are some constants.

Therefore, we under Assumption 3, we have

$$\Pi(\|\beta - \beta^*\|_1 < \delta) \geq \Pi(\|\beta - \beta^*\|_1 < \delta \mid E_\tau)\Pi(E_\tau) \geq (1 - C'/(nT))^{T-s} K'' e^{-Ms \log(nT)} \geq e^{-K^*s \log(nT)},$$

where K^* is a positive constant. □

7.11 Proof of Lemma 4.1

Proof.

$$[\mathbf{E}(\mathbf{D}(\mathbf{a})\Xi\mathbf{D}(\mathbf{a}))]_{ij} = \mathbf{E}(a_i\Xi_{ij}a_j) = \begin{cases} \mu_i\Xi_{ij}\mu_j + \Xi_{ij}\Sigma_{ij} & \text{if } i \neq j, \\ \mu_i\Xi_{ij}\mu_i + \Xi_{ij}\Sigma_{ii} & \text{if } i = j. \end{cases}$$

□

Proposition 7.1. *The equation (21) is satisfied for $\tau \sim \text{Ca}^+(0, 1)$ and $\tau^2 \sim \text{Gamma}(a_\tau, b_\tau)$ with positive constants a_τ, b_τ .*

Proof. Given $\tau \sim \text{Ca}^+(0, 1)$, for any $s = 1, \dots, T$, by mean-value theorem, we have

$$g(\tau^* < \tau < 2\tau^*) = \int_{\tau^*}^{2\tau^*} \frac{1}{1+\tau^2} d\tau \geq \tau^* \geq c_1 e^{-c_2 s \log(nT)},$$

where the final inequality follows by $\log(\tau^*) \gtrsim -s \log(nT)$, and c_1, c_2 are positive constants. Given the $\Gamma(a_\tau, b_\tau)$ prior for τ^2 with constants a_τ, b_τ , for any $s = 1, \dots, T$, by mean-value theorem,

$$\begin{aligned} g(\tau^* < \tau < 2\tau^*) &= \int_{\tau^{*2}}^{4\tau^{*2}} \frac{b_\tau^{a_\tau}}{\Gamma(a_\tau)} \tau^{2(a_\tau-1)} e^{-b_\tau \tau^2} d\tau^2 \geq c_1 \tau^{*(2a_\tau-2)} e^{-c_2 \tau^{*2}} \tau^{*2} \\ &\geq c_1 e^{-c_2 \tau^{*2} + 2a_\tau \log \tau^*} \geq c_1 e^{-c_3 s \log(nT)}, \end{aligned}$$

where the final inequality follows by $-\tau^{*2} \gtrsim -s \log(nT)$ and $\log(\tau^*) \gtrsim -s \log(nT)$, and c_1, c_2, c_3 are positive constants. \square

Lemma 7.5 (Perturbation bound for procrustes, Theorem 1 in [Arias-Castro et al. \(2020\)](#)). *Consider two matrices $\mathbf{X}, \mathbf{Y} \in \mathbb{R}^{n \times d}$, with \mathbf{X} having full rank, and set $\epsilon^2 = \|\mathbf{Y}\mathbf{Y}^T - \mathbf{X}\mathbf{X}^T\|_F$. Then if $\|\mathbf{X}^\dagger\|_F \leq 1/\sqrt{2}$, we have*

$$\min_{\mathbf{O} \in \mathbb{O}^{d \times d}} \|\mathbf{Y} - \mathbf{X}\mathbf{O}\|_F \leq (1 + \sqrt{2}) \|\mathbf{X}^\dagger\|_F \epsilon^2, \quad (24)$$

where \mathbf{X}^\dagger is the pseudo-inverse of \mathbf{X} .

Lemma 7.6 (K -means error bound, adapted from Lemma 5.3 in [Lei and Rinaldo \(2015\)](#)). *For any two matrices $\hat{\mathbf{U}}, \mathbf{U} \in \mathbb{R}^{n \times d}$ such that $\mathbf{U} = \mathbf{\Theta}\mathbf{X}$ with $\mathbf{\Theta} \in \mathbb{M}_{n,K}$, $\mathbf{X} \in \mathbb{R}^{K \times d}$, let $(\hat{\mathbf{\Theta}}, \hat{\mathbf{X}})$ be the solution to the K -means problem and $\bar{\mathbf{U}} = \hat{\mathbf{\Theta}}\hat{\mathbf{X}}$. Then for any $\delta_k \leq \min_{l \neq k} \|\mathbf{u}_l - \mathbf{u}_k\|_2$, define $S_k = \{i \in G_k(\mathbf{\Theta}) : \|\bar{\mathbf{u}}_i - \mathbf{u}_i\|_2 \geq \delta_k/2\}$, then*

$$\sum_{k=1}^K |S_k| \delta_k^2 \leq 16 \|\hat{\mathbf{U}} - \mathbf{U}\|_F^2.$$

Moreover, if

$$16 \|\hat{\mathbf{U}} - \mathbf{U}\|_F^2 / \delta_k^2 < n_k \quad \text{for all } k,$$

then there exists a $K \times K$ permutation matrix J such that $\hat{\mathbf{\Theta}}_{G^*} = \mathbf{\Theta}_{G^*} J$, where $G = \bigcap_{k=1}^K (G_k - S_k)$.

7.12 CAVI algorithm

First, given $q(\theta)$, the updating of $q(\beta)$ is as follows:

$$q(\beta) \propto \exp[\mathbf{E}_{-\beta} \{\log p_\alpha(\theta, \beta, \mathcal{Y})\}] \propto \exp[\mathbf{E}_\theta \{\log P_\alpha(\mathcal{Y} \mid \theta, \beta)\} + \log p(\beta)],$$

which has a closed-form expression when the likelihood and priors are in a Gaussian form.

Given the above moment of λ_{it} , τ_i and σ_{0i} , the updating of $q(\theta_{i\cdot})$ can be obtained through the message-passing framework: suppose $q(\beta)$, $q(\tau)$, $q(\sigma_0)$ and $q_j(\theta_{j\cdot})$, $j \neq i$ are given and the target is to update $q_i(\theta_{i\cdot})$, we have:

$$q_i(\boldsymbol{\theta}_{i\cdot}) \propto \exp \left[\mathbf{E}_{-\boldsymbol{\theta}_{i\cdot}} \left\{ \sum_{t=1}^T \sum_{j \neq i, j=1}^n \{ \log P_\alpha(Y_{ijt} \mid \boldsymbol{\theta}_{it}, \boldsymbol{\theta}_{jt}, \beta) \} \right. \right. \\ \left. \left. + \sum_{t=1}^{T-1} \log p(\boldsymbol{\theta}_{i(t+1)} \mid \boldsymbol{\theta}_{it}, \lambda_{it}) + \log p(\boldsymbol{\theta}_{i1} \mid \sigma_{0i}) \right\} \right], \quad (25)$$

where $\mathbf{E}_{-\boldsymbol{\theta}_{i\cdot}}$ is the expectation taken with respect to the density $[\prod_{j \neq i} q_j(\boldsymbol{\theta}_{j\cdot})]q(\beta)q(\boldsymbol{\Lambda})q(\boldsymbol{\sigma}_0)$.

We have the following factorial property for fractional joint distribution $p_\alpha(\mathcal{Y}, \Theta, \beta, \mathbf{H}, \boldsymbol{\Lambda}, \boldsymbol{\tau}, \boldsymbol{\sigma}_0)$:

$$p_\alpha(\mathcal{Y}, \Theta, \beta, \mathbf{H}, \boldsymbol{\Lambda}, \boldsymbol{\tau}, \boldsymbol{\sigma}_0) \\ \propto P_\alpha(\mathcal{Y} \mid \Theta, \boldsymbol{\Lambda}, \boldsymbol{\tau}, \beta, \boldsymbol{\sigma}_0, \mathbf{H})p(\Theta \mid \boldsymbol{\Lambda}, \boldsymbol{\tau}, \boldsymbol{\sigma}_0)p(\boldsymbol{\Lambda} \mid \mathbf{H})p(\mathbf{H})p(\beta)p(\boldsymbol{\tau}) \\ = \prod_{i=1}^n \left\{ \prod_{t=1}^{T-1} p(\boldsymbol{\theta}_{i(t+1)} \mid \boldsymbol{\theta}_{it}, \lambda_{it}, \tau_i)p(\lambda_{it} \mid \eta_{it})p(\eta_{it})p(\boldsymbol{\theta}_{i1} \mid \sigma_{0i}) \right\} p(\beta)p(\boldsymbol{\tau}_i) \quad (26) \\ \times \prod_{t=1}^T \prod_{1 \leq i \neq j \leq n} P_\alpha(Y_{ijt} \mid \boldsymbol{\theta}_{it}, \boldsymbol{\theta}_{jt}, \beta),$$

with $p(\boldsymbol{\theta}_{i(t+1)} \mid \boldsymbol{\theta}_{it}, \lambda_{it}, \tau_i) \propto \exp(-\|\boldsymbol{\theta}_{i(t+1)} - \boldsymbol{\theta}_{it}\|_2^2 / (2\tau_i^2 \lambda_{it}^2))$ for $t = 1, \dots, T-1$.

By the scheme of CAVI, given the distributions $q(\Theta), q(\beta)$, we have updatings of $\lambda_{it}, \eta_{it}, \sigma_{0i}$:

$$\hat{q}(\lambda_{it}, \eta_{it}, \sigma_{0i}) \propto \exp[\mathbf{E}_{-\lambda_{it}, \eta_{it}, \sigma_{0i}} \{ \log p_\alpha(\mathcal{Y}, \Theta, \beta, \mathbf{H}, \boldsymbol{\Lambda}, \boldsymbol{\tau}, \boldsymbol{\sigma}_0) \}] \\ \propto \exp[\mathbf{E}_{-\lambda_{it}, \eta_{it}, \sigma_{0i}} \{ \log P(\Theta \mid \boldsymbol{\sigma}_0, \boldsymbol{\Lambda}) + \log P(\boldsymbol{\Lambda} \mid \mathbf{H}) + \log P(\mathbf{H}) + \log p(\boldsymbol{\sigma}_0) \}] \\ \propto \exp \left[-\frac{d+3}{2} \log(\lambda_{it}^2) - \mathbf{E}_{\boldsymbol{\theta}_{i\cdot}} \left\{ \frac{\|\boldsymbol{\theta}_{it} - \boldsymbol{\theta}_{i(t+1)}\|_2^2}{2\tau_i^2 \lambda_{it}^2} \right\} - 2 \log(\eta_{it}^2) - \frac{1}{\eta_{it} \lambda_{it}^2} - \frac{1}{\eta_{it}} \right. \\ \left. - \mathbf{E}_{x_{i1}} \left(\frac{\|\boldsymbol{\theta}_{i1}\|_2^2}{2\sigma_{0i}^2} \right) - \left(\frac{d}{2} + a_{\sigma_0} + 1 \right) \log(\sigma_0^2) - \frac{b_{\sigma_0}}{\sigma_{0i}^2} \right].$$

Therefore, we have

$$\eta_{it}^{(new)} \sim \text{IG} \left(1, 1 + \mu_{1/\lambda_{it}^2} \right); \\ \lambda_{it}^{2(new)} \sim \text{IG} \left(\frac{d+1}{2}, \mu_{1/\eta_{it}} + \mathbf{E}_{\boldsymbol{\theta}_{it}, \boldsymbol{\theta}_{i(t+1)}} \left[\frac{\|\boldsymbol{\theta}_{it} - \boldsymbol{\theta}_{i(t+1)}\|_2^2}{2\tau_i^2} \right] \right); \quad (27) \\ \sigma_{0i}^{2(new)} \sim \text{IG} \left(\frac{nd + a_{\sigma_0}}{2}, \frac{\mathbf{E}_{q(\boldsymbol{\theta}_{i1})}(\|\boldsymbol{\theta}_{i1}\|_2^2) + 2b_{\sigma_0}}{2} \right),$$

where $\mu_{1/\lambda_{it}^2} = \mathbf{E}_{q(\lambda_{it})}(1/\lambda_{it}^2)$ and $\mu_{1/\eta_{it}} = \mathbf{E}_{q(\eta_{it})}(1/\eta_{it})$. Note that the key moment has a closed-form expression in terms of the parameters: $a \sim \text{IG}(\alpha, \beta)$, $\mathbf{E}(1/a) = \alpha/\beta$.

Given the equation (25), note that $q_i(\boldsymbol{\theta}_{i\cdot})$ has the following form:

$$q_i(\boldsymbol{\theta}_{i\cdot}) = q_{i1}(\boldsymbol{\theta}_{i1}) \prod_{t=1}^{T-1} q(\boldsymbol{\theta}_{i(t+1)} | q(\boldsymbol{\theta}_{it})) = \prod_{t=1}^{T-1} \frac{q_{it,i(t+1)}(\boldsymbol{\theta}_{it}, \boldsymbol{\theta}_{i(t+1)})}{q_{it}(\boldsymbol{\theta}_{it})q_{i(t+1)}(\boldsymbol{\theta}_{i(t+1)})} \prod_{t=1}^T q_{it}(\boldsymbol{\theta}_{it}). \quad (28)$$

It follows that the graph of random variable $\boldsymbol{\theta}_i$ is structured by a chain from $\boldsymbol{\theta}_{i1}$ to $\boldsymbol{\theta}_{iT}$. Due to the above structure (28), the computation of $q_i(\boldsymbol{\theta}_{i\cdot})$ given the rest densities can be carried out efficiently in a message-passing manner. In particular, the message-passing algorithm involves computing all the unary marginals $\{q_{it}\}$ and binary marginals $\{q_{it,i(t+1)}\}$, which in turn help to update scales in closed forms (27).

When Gaussian likelihood is adopted:

$$P_\alpha(\mathcal{Y} | \Theta, \beta) = \prod_{t=1}^T \prod_{1 \leq i \leq n, 1 \neq j \leq p} \frac{1}{\sqrt{2\pi}\sigma} \exp \left[-\alpha \frac{\{Y_{ijt} - \mathbf{u}'_{it} \mathbf{v}_{jt}\}^2}{2\sigma^2} \right].$$

where σ is the β in the previous general setting, the MP updating can be implemented in the framework of Gaussian belief propagation networks, where the mean and covariance of the new update of variational distribution can be calculated by Gaussian conjugate and marginalization using the Schur complement. In addition, the updating of σ can also be obtained in the closed forms via inverse-gamma conjugacy.

For the Bernoulli likelihood:

$$P_\alpha(Y_{ijt} | \mathbf{u}_{it}, \mathbf{v}_{jt}) = \exp[\alpha Y_{ijt}(\mathbf{u}'_{it} \mathbf{v}_{jt}) - \alpha \log\{1 + \exp(\mathbf{u}'_{it} \mathbf{v}_{jt})\}].$$

The tangent transform approach proposed by Jaakkola and Jordan (2000) is applied in the present context to obtain closed-form updates.

By introducing $\Xi = \{\xi_{ijt} : i, j = 1, \dots, n, t = 1, \dots, T\}$ with $A(\xi_{ijt}) = -\tanh(\xi_{ijt}/2)/(4\xi_{ijt})$ and $C(\xi_{ijt}) = \xi_{ijt}/2 - \log(1 + \exp(\xi_{ijt})) + \xi_{ijt}\tanh(\xi_{ijt}/2)/(4\xi_{ijt})$ for any ξ_{ijt} , the following lower bound on $P_\alpha(Y_{ijt} | \mathbf{u}_{it}, \mathbf{u}_{jt}, \beta)$ holds:

$$\underline{P}_\alpha(Y_{ijt} | \mathbf{u}_{it}, \mathbf{v}_{jt}; \xi_{ijt}) = \exp \left[\alpha A(\xi_{ijt})(\mathbf{u}'_{it} \mathbf{v}_{jt})^2 + \alpha \left(Y_{ijt} - \frac{1}{2} \right) (\mathbf{u}'_{it} \mathbf{v}_{jt}) + \alpha C(\xi_{ijt}) \right].$$

The likelihood $P_\alpha(Y_{ijt} | \mathbf{u}_{it}, \mathbf{u}_{jt})$ is replaced by its lower bound $\underline{P}_\alpha(Y_{ijt} | \mathbf{u}_{it}, \mathbf{v}_{jt}; \xi_{ijt})$, where the updating of Θ in the Gaussian conjugate framework can be performed. After updating all the variational densities, ξ_{ijt} is optimized based on EM algorithm according to Jaakkola and Jordan (2000): $\xi_{ijt}^{(new)} = \mathbf{E}_{q(\Theta)}\{(\mathbf{u}'_{it} \mathbf{v}_{jt})^2\}$. To summarize, for Gaussian or Bernoulli likelihoods, the proposed variational framework allows all updating in the Gaussian conjugate paradigm by assuming only independent relationships between different subjects within the variational family.